1-1-2015

Virtual Polytopes

G. Yu Panina
Saint Petersburg State University

I. Streinu
Smith College, istreinu@smith.edu

Recommended Citation

Virtual Polytopes

Gaiane Panina [1] and Ileana Streinu [2]

February 14, 2015

Abstract

Originating in diverse branches of mathematics, from polytope algebra and toric varieties to the theory of stressed graphs, virtual polytopes represent a natural algebraic generalization of convex polytopes. Introduced as the Grothendick group associated to the semigroup of convex polytopes, they admit a variety of geometrizations. A selection of applications demonstrates their versatility.

1 Introduction

Convex polytopes in the Euclidean space form a semigroup with respect to Minkowski addition. This semigroup is not a group, since, in most cases, the Minkowski difference of two polytopes is not convex. But the cancellation law holds, and this allows for the unique extension of the semigroup to the Grothendick group: this is, by definition, the *group of virtual polytopes*. From a purely algebraic point of view, virtual polytopes are a most natural generalization of convex polytopes: in short, a virtual polytope is defined as a *formal Minkowski difference of convex polytope*.

The first goal of this survey is to bridge the gap between this formal, algebraic definition and various interesting geometric interpretations. The second goal is to present different applications of the geometrization machinery, insights into the diverse questions that motivated their study, and to set up an appropriate framework for problems lying beyond this theory.

The main message that will emerge is that virtual polytopes retain the structure and many properties of convex polytopes, except convexity: a virtual polytope has a well defined face lattice, support function, outer normal fan, volume,

---
[1] St. Perersburg State University, Institute for Informatics and Automation, V.O. 14 line 39, St.Petersburg, 199178, Russia. gaiane-panina@rambler.ru

[2] Department of Computer Science, Smith College, Northampton, MA 01063, USA. istreinu@smith.edu,http://cs.smith.edu/~streinu. Supported by NSF grants CCF-1016988 and CCF-1319366.

lattice points enumeration concept, etc. However, the support function is no longer convex, the volume can be negative, the outer normal fan can contain non-convex cones, etc.

It is not unusual in mathematics that different formalisms lead to essentially equivalent concepts: homology theories, (oriented) matroids, combinatorially rigid structures, abstract polytopes, etc. have a multitude of crypto-morphic definitions, each with its own abstract structure and a set of axioms or consistency rules to be satisfied. Each is motivated by a concept arising perhaps in another part of mathematics, and each time there are rules for converting from one formalism to the other.

Virtual polytopes also fit this pattern. As generalizations of convex polytopes, they will be described as piecewise constant functions, collections of translated cones, piecewise linear functions, invertible sheaves on a toric variety and, in lower dimensions, stressed graphs on the unit sphere or special types of 2D polygonal chains. In each setting we have one and the same group of virtual polytopes[5], up to a canonical isomorphism.

Specifically, for each of the representations we describe a group of geometric objects which turns out to be canonically isomorphic to the group of virtual polytopes. Canonical isomorphisms between all the representations appear automatically: we go from one representation to the group of virtual polytopes, and from there to the other representation. However, in many situations direct isomorphisms appear naturally between some of these representations.

Historical perspective. The first systematic study of virtual polytopes, referred to with this very name, appears in A.G. Khovanski and A.V. Puklikhov's paper [19]. They work is motivated by the algebraic geometry of toric varieties[6]. It was known that invertible bundles on a projective toric variety form a group (the Picard group); it was also known that very ample bundles correspond to convex polytopes (and form a semigroup), so the natural question arose: *"what corresponds geometrically to the other elements of the Picard group, i.e. to bundles that are not ample?"*. Some technical details aside, the answer is: *"The Picard group is isomorphic to the group of virtual polytopes"*. A more extended discussion appears in G. Ewald's book [12].

The idea of Minkowski subtraction of convex polytopes and convex sets can be traced back even further. In an early paper from 1939, A.D. Alexandrov [1] considered pointwise differences of support functions. Although not explicitly stated in his paper, this point of view leads to another way of defining virtual polytopes, which we describe in Section 4.3.

Another important observation comes from the work of H. Grömer [14], who wrote in 1977: *"It appears that an addition of non-convex sets ... must neces-*

---

[5]The precise definition and further details appear in Section 2.
[6]We present this as an application in Section 6.5.

2

sarily take into account multiplicities of points, and this leads immediately to functions instead of ordinary sets." He also wrote: "*It turns out that Minkowski addition is actually more akin to multiplication in a certain algebra than to addition.*" We discuss this in Section 4.1.

More recently and in a different context, L. Rodriguez and H. Rosenberg [41] introduced a class of polyhedral surfaces, called *polyhedral hedgehogs*[7], which turn out to be a subclass of virtual polytopes. Subsequently, V. Alexandrov studied polyhedral hedgehogs in [2]. We present a similar (but not identical) construction which covers the entire set of virtual polytopes in Sections 5. Y. Martinez-Maure studied various aspects of hedgehogs and gave a sketch of an inductive definition (by dimension) of virtual polytopes in [23]. In Section 5, we present an approach inspired, partially, by his ideas.

Virtual polytopes also appeared, implicitly, in P. McMullen's polytope algebra [26]. In section 4.2, we extract from his algebraico-geometric formalism the aspects relevant to the theory of virtual polytopes.

An important warning.   The theory of virtual polytopes is built upon an appropriate notion of *Minkowski subtraction*, but care must be exercised even with this most primitive ingredient. Indeed, various other definitions have appeared in the literature. For instance, the concept of Minkowski difference, as described in R. Schneider's book [43], is not the same as what we present in Section 2. The problem is that Schneider's straightforwad definition of Minkowski subtraction does not turn the semigroup of convex polytopes into a group: in his theory, $P - P \neq 0$.

Overview of the survey.   We start in Section 2 with the basic definitions, and treat virtual polytopes as formal Minkowski differences. Important properties can already be defined in this setting; in particular we introduce *faces of virtual polytopes.*

The first non-trivial geometrization is described in Section 3 for two-dimensional virtual polytopes: we represent them as *colored polygons*. This kind of "toy" representation is very intuitive but is possible only in dimension two.

Section 4 presents four types of geometrizations that work in all dimensions: (1) piecewise constant functions, which are elements of A. Khovanskii and A. Pukhlikov's algebra, (2) elements of the first weight space of P. McMullen's polytope algebra, (3) support functions, and (4) systems of translated cones.

We return to lower dimensions in Section 5, where we present an approach based on rigidity theory. Here a virtual polytope appears as a system of springs in equilibrium on the sphere. A more intuitive representation is then done via what

---

[7]In French, *hérissons.*

3

we call *Maxwell polytopes*, which are geometrizations of closed polyhedral surfaces whose faces are flat polygons which may not be convex; even worse, these faces, as well as the whole "surface", may have self-intersections and exhibit other types of unusual features.

We conclude in Section 6 with several applications for virtual polytopes. We discuss here: (1) generalizations of A.D. Alexandrov-type problems for convex bodies and convex polytopes, (2) volumes and mixed volumes of virtual polytopes, (3) Minkowski decompositions of polytopes, and (4) the relationship to algebraic toric geometry.

2 Main Definition

In this section we define virtual polytopes as formal Minkowski differences of convex polytopes and state some important properties that follow directly from the definition.

2.1 Convex polytopes and Minkowski summation

Throughout the paper, we assume that the ambient space for all our constructions is the Euclidean space $\mathbb{R}^d$ with a fixed Cartesian coordinate system and the standard scalar product denoted with $\langle x, y \rangle$.

Convex Polytopes. A *convex polytope* is the convex hull of a non-empty finite point set in some $\mathbb{R}^d$. When there is no risk of confusion, we may drop "convex" and use the shorter term *"polytope"*. The set of all convex polytopes in $\mathbb{R}^d$ is denoted by $\mathcal{P}_d$. To keep the notation simple, we omit the "d" and use $\mathcal{P} := \mathcal{P}_d$. However we emphasize that we always work in a fixed ambient space.

The *dimension* of a convex polytope K is the dimension of its *affine hull*, which is the (minimal by inclusion) affine plane containing K. Thus the dimension of a convex polytope in $\mathbb{R}^d$ is not necessarily d; in particular, the polytope can be the degenerate zero-dimensional *single point polytope*.

Minkowski addition of convex polytopes. From two convex polytopes K and L, the operation of Minkowski addition generates a new convex polytope $K \otimes L$ defined by the pairwise addition of the points in the two sets:

$$K \otimes L = \{x + y \mid x \in K, y \in L\}.$$

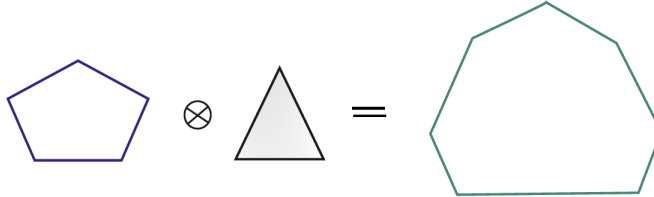An example in the plane is shown in Figure 1.

Figure 1: Minkowski sum of a pentagon and a triangle.

A remark on notation. Most of the literature on Minkowski summation uses the additive notation $+$ or $\oplus$. It was however recognized, in the context of the polytope algebra, that this operation behaves more like multiplication than addition. For this reason, various multiplicative symbols have been employed: $\times$ in [14], $*$ in [19], and "$\cdot$" in [26]. Here, we adopt the multiplicative $\otimes$ notation, in order to be consistent with its multiplicative role in the polytope algebra defined in Section 4.1, and to emphasize its relationship with the tensor product of invertible bundles described in Section 6.5.

Properties of the Minkowski sum. The following basic properties set the foundation for the theory surveyed in this paper:

1. The sum of a polytope K with a point p is a translation of the polytope K by the vector p, which we write as $K + p$.

2. The operation of Minkowski addition allows to factor out translations. That is, for p_1 and p_2, we have:

   $(K_1 + p_1) \otimes (K_2 + p_2) = (K_1 \otimes K_2) + (p_1 + p_2).$

3. **(Cancellation law)** If $K \otimes L = K' \otimes L$ then $K = K'$.

With a few (explicitly stated) exceptions, we will **factor out translations**, i.e., we will identify a polytope K and its translate $K + p$.

The operation of Minkowski addition turns the set $\mathcal{P}$ of convex polytopes, factored by translations, into a commutative semigroup in which the above cancellation law holds. The **unit element** E is the convex polytope containing exactly one point. Since all such polytopes differ by a translation, we may assume that the unit element is represented by the origin: $E = \{O\}$.

2.2 Virtual polytopes as Grothendieck groups

Grothendieck group: the general construction. Whenever we have a commutative semi-group S (whose operation we denote multiplicatively) with a unit element e, it can be extended to a group iff it satisfies the cancellation law:

$$kl = ml \quad \text{implies that} \quad k = m$$

The unique minimal abelian group containing S as a sub-semigroup, up to isomorphism, is called *the Grothendick group of S*. Its elements are equivalence classes of formal expressions (or *formal fractions*) kl^{-1}, with $k, l \in S$, identified by the the following rule: two formal expressions $k_1 l_1^{-1}$ and $k_2 l_2^{-1}$ are identified whenever $k_1 l_2 = k_2 l_1$.

The elements k of the semigroup are identified with fractions ke^{-1}.

An elementary example of this construction is the group of non-zero rational numbers under multiplication, which extends the semi-group of non-zero integers. Using this analogy, the convex polytopes will be our "integers", while the virtual polytopes will correspond to the "rational numbers".

Virtual polytopes: main definition. The discussion in the previous paragraph justifies the following:

Definition 1. *The group $\mathcal{P}^*$ of virtual polytopes is the Grothendick group associated to the semigroup $\mathcal{P}$ of convex polytopes under Minkowski addition.*

The inverse in this group of a convex polytope K is denoted by $K^{\otimes -1}$. For further reference, we list a few simple but useful consequences of the definition:

1. A virtual polytope is a formal fraction $K \otimes L^{\otimes -1}$.

2. Two virtual polytopes represented by expressions $K_1 \otimes L_1^{\otimes -1}$ and $K_2 \otimes L_2^{\otimes -1}$ are identified whenever $K_1 \otimes L_2 = K_2 \otimes L_1$.

3. The group operation literally repeats the rules of multiplication of two fractions. That is, we define

$$(K_1 \otimes L_1^{\otimes -1}) \otimes (K_2 \otimes L_2^{\otimes -1}) := (K_1 \otimes K_2) \otimes (L_1 \otimes L_2)^{\otimes -1}.$$

4. The unit element is represented by $E \otimes E^{\otimes -1}$, where E is the unit element in $\mathcal{P}$, that is, the one-point polytope. The unit element also may be represented by any $K \otimes K^{\otimes -1}$.

The natural inclusion of convex polytopes into the group of virtual polytopes:

$$\mathcal{P} \hookrightarrow \mathcal{P}^*$$

takes a convex polytope $K \in \mathcal{P}$ to the formal fraction $K_1 \otimes E^{\otimes -1}$.

Dimension of a virtual polytope.   Since a virtual polytope is not a pointset, the concept of *dimension* requires some care. We define the *dimension of a virtual polytope P* to be the smallest number k such that P can be expressed as $P = K \otimes L^{\otimes -1}$, with K and L convex polytopes lying in the same k-dimensional subspace of $\mathbb{R}^d$.

In geometric representations of virtual polytopes, the dimension will correspond to its geometrical counterpart: as expected, a k-dimensional polytope will be represented by a k-dimensional geometrical object.

Various geometric realizations of virtual polytopes are presented in subsequent sections. As a warm-up, we discuss now briefly the simplest cases, in dimensions zero and one[8].

Virtual polytopes in dimension zero.   This is the trivial group with only one element (the unit element E), which corresponds, geometrically, to the unique zero-dimensional polytope.

Virtual polytopes in dimension one.   A convex polytope in $\mathbb{R}^1$ is a segment. After factoring out the translations, we can identify a segment with a positive real number: its length. In this setting, the Minkowski addition of segments amounts to addition of positive real numbers. Thus, the semigroup of convex polytopes $\mathcal{P}$ in $\mathbb{R}^1$ is isomorphic to the semigroup $\mathbb{R}_{\geq 0}$ of non-negative real numbers with the group operation "+". The semigroup isomorphism maps a segment to its length. This implies that the group of virtual segments $\mathcal{P}^*$ is isomorphic to $\mathbb{R}$.

For further reference, we state explicitly the *three types of virtual segments*:

- The segment of zero length, i.e., a one-point polytope. It is the unit element E.

- Segments of positive lengths, that is, usual convex segments, and

- Inverses (in the sense of Minkowski addition) of convex segments.

The inverses of convex segments may be conceived as having an associated negative sign, but a more intuitive convention makes use of *colors* instead of *signs*.

Virtual 1D polytopes as colored segments.   A simple visual representation of virtual segments is obtained by *coloring* regular segments: the convex segments (which correspond to positive numbers) are colored in red. Their inverses (corresponding to negative numbers) are represented by convex segments colored in blue. This way of visualizing virtual segments will be used in the next section for colored stars and polygons, and form the basis of an inductive construction leading to virtual polytopes in higher dimensions.

---

[8]We refer to one, two and three-dimensional objects as being in 1D, 2D and 3D.

For further reference, we formulate now the Minkowski addition $\otimes$ of virtual segments in terms of colored segments:

- the sum of two segments of the same color has length equal to the sum of the lengths of the summands, and inherits the color;

- two segments of different colors and equal length add up to the one-point segment, and

- two segments of different colors add up to a segment whose color is inherited from the longer of the two segments, and whose length is the difference of the two lengths. In particular, the inverse of a colored segment is a segment of the same length and opposite color.

An example for two convex segments K and L is shown in Figure 2: the Minkowski difference $K \otimes L^{-1}$ is a convex segment, and therefore is colored red; its inverse, the Minkowski difference $L \otimes K^{-1}$, is colored blue.
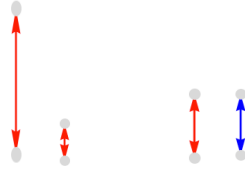

Figure 2: Two 1D convex polytopes (segments) K and L and their Minkowski differences $K \otimes L^{\otimes -1}$ and $L \otimes K^{\otimes -1}$.

2.3 Facial structure of virtual polytopes

Virtual polytopes, just like the convex ones, have a well defined facial structure. We start by reviewing a few important properties of faces of convex polytopes. Many of them carry through to virtual polytopes, except topology and convexity.

Faces of convex polytopes. Let K be a convex polytope in dimension d. For a given direction vector $v \in \mathbb{R}^d$, the *face K^v of K in the direction v* is the set of points p where the scalar product $\langle v, . \rangle$ attains its maximum value, over all points $p \in K$. When $v = 0$, we get $K^v = K$. Otherwise, K^v is the intersection of K with the support hyperplane to K whose outer normal vector is v.

Theorem 1. *Faces of convex polytopes satisfy the following properties [12]:*

- ***Convexity of faces:*** *A face of a convex polytope is a convex polytope.*

- ***"To be a face" is a hereditary property:*** *a face of a face of a convex polytope K is itself a face of K.*

8

- **Faces behave additively:** *A face in the direction v of a Minkowski sum $K \otimes L$ is the Minkowski sum of the faces in direction v of the summands:*

$$(K \otimes L)^v = K^v \otimes L^v.$$

The faces of a convex polytope, ordered by inclusion[9], form a partially ordered set called the *face lattice*. The face lattice captures the connectivities between faces of all dimensions, and contains information about the combinatorics and topology of the polytope.

We turn now to a preliminary discussion of the facial structure for virtual polytopes. Concrete examples, geometric interpretations and specific properties are interspersed throughout the rest of the paper.

Faces of virtual polytopes. For a given direction vector v, we have a semigroup homomorphism $K \rightarrow K^v$ taking convex polytopes from $\mathbb{R}^n$ to convex polytopes lying in the corresponding hyperplane H^v with v as normal vector. In [33] it was shown that this map has a unique extension to a group homomorphism.

This allows us to define the *face of P in the direction v* of a virtual polytope P as the image P^v of K by this unique group homomorphism. As an immediate consequence, we have the following explicit formulation:

Definition 2. *Let $P = K \otimes L^{\otimes -1}$ be a virtual polytope, where K and L are convex polytopes, and v be a direction vector. The face P^v is defined as*

$$P^v = K^v \otimes (L^v)^{\otimes -1}$$

This definition makes possible an analog of Theorem 1.

Theorem 2. *Faces of virtual polytopes satisfy the following properties [33]:*

- **Faces are "virtual":** *A face of a virtual polytope is a virtual polytope.*

- **"To be a face" is a hereditary property:** *A face of a face of a virtual polytope P is itself a face of P.*

- **Faces behave additively:** *A face in the direction v of a Minkowski sum of two virtual polytopes is the Minkowski sum of the faces in direction v from the summands: $(K \otimes L)^v = K^v \otimes L^v$.*

The theorem allows us to introduce in a natural way a partial order on the set of faces, where a face F of a virtual polytope P is *smaller* than a face F' of the same virtual polytope P whenever F is a face of F'. The faces can be ranked by dimension. As usual, a k-dimensional face is shortly referred to as a *a k-face*, 0-faces are called *vertices*, 1-faces are *edges* and the $(d-1)$-faces are *facets*.

With these preliminaries in place, we turn to a detailed investigation of the 2D case.

---

[9]For convex polytopes, face inclusion $F < F'$ means that face F is a subset of face F'.

3 Virtual polygons

This section is devoted to the first non-trivial example of virtual polytopes: the 2D virtual polygons. Because convex polygons have very simple representations, we can quickly introduce the concepts leading to their "virtualization". This is not just a useful exercise to build up the intuition of what a virtual polytope might be, but it also covers the basic cases of an inductive construction that will be presented later in Section 5.

3.1 Preliminaries: polygons, stars and weighted units

We start by making precise, fixing the notation and illustrating simple correspondences between a few basic concepts used throughout the paper: polygons and stars, convex polygons and their Minkowski sums.
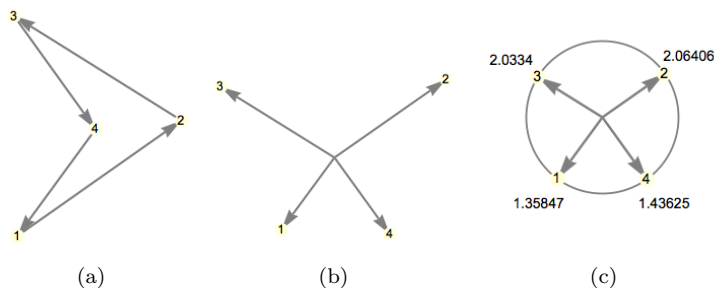

Figure 3: (a) An oriented polygon, (b) its associated balanced star and (c) associated weighted units.

Polygons. A *polygon* is a cyclically ordered set of points in the plane $P = \{p_1, \cdots, p_n\}$ so that either $n = 1$ or consecutive points p_i and p_{i+1} are pairwise distinct[10]. The cyclical ordering of the points means that we consider two polygons to be identical if one is obtained from the other by a cyclic permutation. In other words, our polygons have an induced orientation, and the reverse orientation yields (in most cases considered in this paper) a different polygon. The consecutive pairs of points determine the edges of the polygon, which have non-zero length. To visualize the cyclic ordering of points, we draw a polygon with its edges oriented in the direction of the underlying cycle (Figure 3). We emphasize from the outset that we work here with arbitrary polygons, which may not be simple: they may self-intersect or have overlapping edges.

---

[10]Index arithmetic is done modulo n in the set $\{1, 2, \cdots, n\}$

Balanced stars. A *star* is a cyclically ordered set of non-zero vectors $V = \{v_1, \cdots, v_n\}$. A star is *balanced* if the vectors sum up to zero:

$$\sum_{i=1}^{n} v_i = 0$$

The *star associated to an arbitrary polygon* is obtained by translating to the origin all the oriented edge vectors $v_i = p_{i+1} - p_i$, as in Figure 3(a,b). The star is balanced, since the edge vectors of a polygon always satisfy the balance equation.

Balanced sets of weighted points on the unit circle. A vector $v \in \mathbb{R}^2$ can be represented in polar coordinates as a pair (α_i, w_i), where $0 \leq \alpha_i < 2\pi$ is the *defining angle* and $w_i > 0$ is the length of the vector, viewed as a positive weight. Each defining angle corresponds to a point on the unit circle S^1. A polygon is thus represented as an arbitrarily ordered set

$$W = \{(\alpha_1, w_1), \cdots, (\alpha_n, w_n)\}$$

of balanced, positively weighted points on the unit circle. An example is shown in Figure 3(c).

Converting between polygon representations. Simple one-to-one correspondences (illustrated in Figure 3) exist between polygons $P = \{p_1, \cdots, p_n\}$ (modulo translations), balanced stars $V = \{v_1, \cdots, v_n\}$ and balanced, positively weighted points on the unit circle. We retain for further reference the two transformations:

- **Polygon-to-star:** The star $V = \{v_1, \cdots, v_n\}$ is defined by the vectors $v_i = p_{i+1} - p_i$, for $i = 1, \cdots, n$.

- **Star-to-polygon:** The polygon $P = \{p_1, \cdots, p_n\}$ is defined by placing p_1 at an arbitrary point in the plane, and the subsequent points as $p_{i+1} = p_i + v_i$.

3.2 Convex polygons as stars and weighted units

For convenience, sometimes both the 2D convex polytope and its boundary will be referred to as a *convex polygon*. For the boundary, we use the convention that it be presented as an ordered set of its extremal points (vertices) $P = \{p_1, \cdots, p_n\}$ *taken in counter-clockwise[11] order*. In other words, as one walks along the polygonal boundary in this order, the interior lies to the left (see Figure 4(a)). We also consider limiting cases such as the *one-vertex polygon* $\{p_1\}$, which has no boundary edges, and the segment-polygon $\{p_1, p_2\}$, whose boundary consists of two parallel edges, with opposite orientations $\overrightarrow{p_1 p_2}$ and $\overrightarrow{p_2 p_1}$.

---

[11] We abbreviate *counter-clockwise* as *ccw*

Convex stars. The *star* associated to a convex polygon has an additional property (illustrated in Figure 4(b)): in the star rotation, the *indices* of the edge vectors appear in the *natural order* $\{1, 2, \cdots, n\}$ induced by the polygon labeling. In general, we say that a star is *convex* if the ccw ordering of its vector labels is the natural order.

Positively weighted units. Similarly, the balanced set

$$W = \{(\alpha_1, w_1), \cdots, (\alpha_n, w_n)\}$$

of weighted points on the circle associated to a convex star is arranged in increasing order of the defining angles $\alpha_1 < \alpha_2 < \cdots < \alpha_n$ (Figure 4(c)). In short, we refer to this representation of a convex polygon as a set of balanced, naturally ordered, positively weighted points on the unit circle as *positively weighted units*.
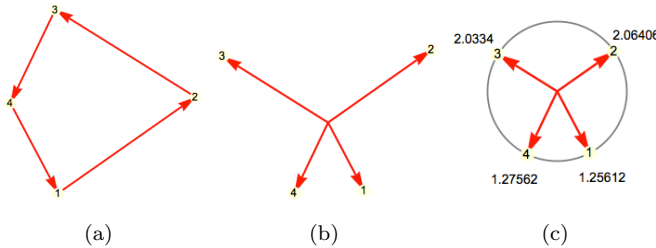

Figure 4: (a) A ccw-oriented convex polygon, (b) its associated, naturally ordered balanced star and (c) its positively weighted circular pointset.

Using the star representation of a convex polygon, the Minkowski sum is computed by the following simple, linear time algorithm (illustrated in Figure 5):

Algorithm: computing the Minkowski sum of two convex polygons.

1. **Polygon-to-star:** Convert the two convex polygons into their convex stars.

2. **Geometric merge:** Merge the two stars (arranged in their natural order) and then add the vectors with the same defining angle.

3. **Star-to-polygon:** Reconstruct a new convex polygon from the resulting star by joining the edge vectors in sequential order.

We remark that, in the second step of the algorithm, the addition of vectors with the same direction and orientation (which differ by a positive scalar) is necessary to ensure that the result is still a convex polygon represented by its extreme points (vertices). This operation is naturally performed using the weighted units representation of the stars. The last step is possible since the sum of the merged set of vectors is still zero.

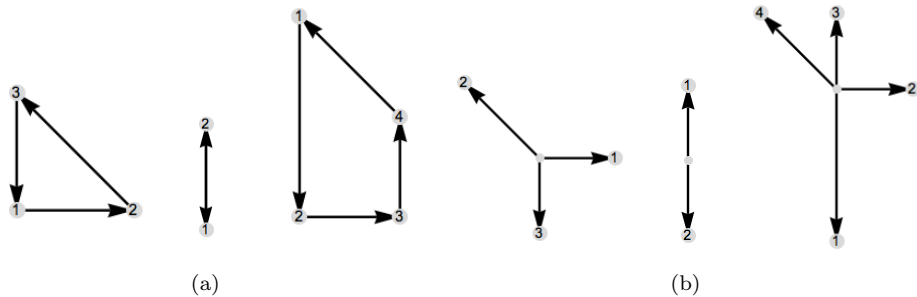With these concepts in place, we are now ready to introduce *virtual polygons*.

<div align="center">(a)   (b)</div>

Figure 5: (a) The Minkowski sum of two convex polygons, and (b) the operation of merging the corresponding convex stars.

3.3 The group of virtual polygons: geometric representations

In this section we present a few concrete, geometric representations of virtual polygons, for which the operation of Minkowski difference will have a naturally defined meaning: *colored balanced stars*, encoded as *balanced weighted units*, and *colored polygons*.

Weighted units. A *weighted unit* is a point on the unit circle, together with a weight, which can be *either positive or negative but not zero*. This information is encoded in a pair (α, w), with $\alpha \in [-\pi, \pi)$ and $w \in \mathbb{R} \setminus \{0\}$. An ordered *balanced set of weighted units* $\{(\alpha_1, w_1), \cdots, (\alpha_n, w_n)\}$ (Figure 6(c)) is defined by the properties:

1. The defining angles are distinct and ccw ordered: $\alpha_1 < \cdots < \alpha_n$.

2. For the vector $v_i \in \mathbb{R}^2 \setminus \{0\}$ with polar coordinates $(\alpha_i, |w_i|)$, $i = 1, \cdots, n$, we have
$$\sum_{i=1}^{n} sign(w_i)v_i = 0.$$

As already observed in the previous section, the convex polygons and the convex stars appear as balanced sets of *positively weighted* units. The empty star corresponds to $n = 0$. We introduce next a convenient visualization of non-empty *virtual* balanced stars, which uses colors and oriented arrows to capture both the cyclic ordering of the weighted units and the orientation that balances the vectors (Figure 6(c)).

Colored star. A weighted unit (α, w) induces an oriented and colored line segment joining the origin with the point on the unit circle corresponding to the defining angle α, defined as follows. If the weight w is positive, the segment

<div align="center">13</div>

is colored red and oriented away from the origin. If the weight w is negative, the color is blue and the orientation is towards the origin. For a balanced set of units, the oriented segments induce a set of balanced vectors. The collection of colored and oriented segments is called a *balanced colored star*, shortly *colored star*. An example is shown in Figure 6(b).
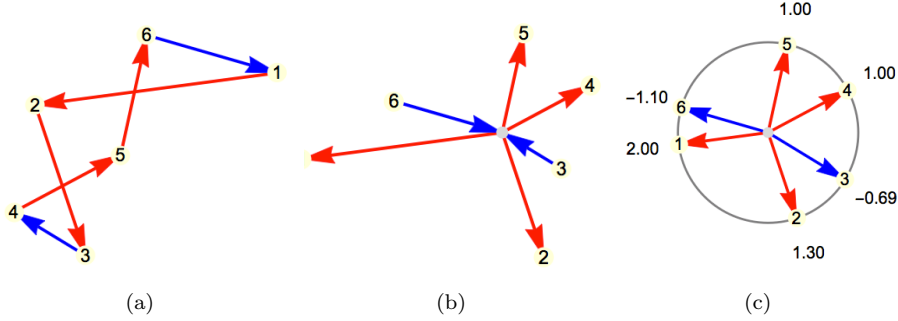

Figure 6: A virtual polygon represented as (a) a colored polygon, (b) a balanced colored star, and (c) a balanced set of weighted units.

We emphasize once again that for a colored star, the numbering of the vectors goes ccw.

A colored star $V = (\{v_1, \cdots, v_n\}, \{c_1, \cdots, c_n\})$ converts to a colored polygon $P = (\{p_1, \cdots, p_n\}, \{c_1, \cdots, c_n\})$ via the following rule:

1. **Coordinates:** Using the **Star-to-polygon** procedure from Section 3.1, we compute the positions $\{p_1, \cdots, p_n\}$ of the polygon vertices from the oriented star vectors $\{v_1, \cdots, v_n\}$

2. **Edge colors:** An edge $p_i p_{i+1}$ retains the color c_i of the star vector v_i.

Since the star is balanced, the algorithm produces a closed polygon.

Definition 3. *A virtual polygon is a polygon $P = \{p_1, \cdots, p_n\}$ whose edges are partitioned into two color classes, **Red** and **Blue** and which is obtained from a balanced colored star via the above conversion.*

A one-point polygon arises from the empty star. Since only edges are colored, there are no colors involved in the one-point polygon.

We now have three sets (weighted units, colored stars, and virtual polygons) together with the conversion rules. Our next step is to introduce group operations such that the conversion rules become group isomorphisms.

Minkowski sum of weighted units. Given two balanced weighted unit vector sets $W' = \{(\alpha'_1, w'_1), \cdots, (\alpha'_n, w'_{n'})\}$ and $W'' = \{(\alpha''_1, w''_1), \cdots, (\alpha''_n, w''_{n''})\}$,
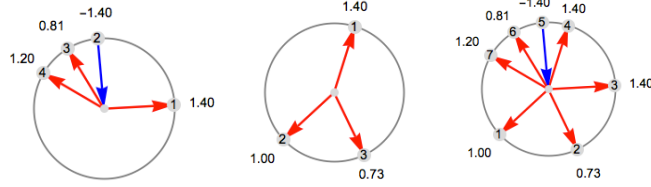
Figure 7: Minkowski sum of two virtual polygons, in the weighted units representation.

their Minkowski sum $W' + W'' = \{(\alpha_1, w_1), \cdots, (\alpha_n, w_n)\}$, with $n \leq n' + n''$ is defined by the following procedure (illustrated in Figure 7):

1. Merge the angle sets $\{\alpha_1', \alpha_2', \cdots, \alpha_{n'}'\}$ and $\{\alpha_1'', \alpha_2'', \cdots, \alpha_{n''}''\}$ to obtain a sorted list of angles, possibly with repetitions.

2. If there are repetitions, i.e. pairs of coinciding angles $\alpha_i' = \alpha_j''$, then add their corresponding weights $w_i' + w_j''$. Otherwise, for position k with angle α_k, retain the weight of the input point it corresponds to.

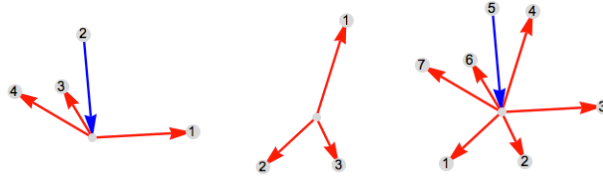3. If a sum $w_i' + w_j''$ equals zero, eliminate the corresponding angle from the list.

Figure 8: Minkowski sum of two virtual polygons, in the colored star representation.

Minkowski sum of colored stars. Given two balanced colored stars, their Minkowski sum (illustrated in Figure 8) is a balanced colored star computed as follows:

1. Merge the stars according to their defining angles.

2. If there are pairs of vectors with the same defining angle, add them up according to the one-dimensional rules. We treat a red vector as a positive (convex) segment and a blue vector as a negative segment. Consequently, the sum is a vector in the same defining angle as the summands, and has a color induced by the magnitudes of the summands.

3. If a sum equals zero, eliminate the corresponding angle from the list.

15

Minkowski sum of virtual polygons. Given two virtual polygons, their sum (Figure 9) is defined via the following algorithm: (a) Take the weighted units of the summands. (b) Add the weighted units. (c) Retrieve a colored polygon from the sum.
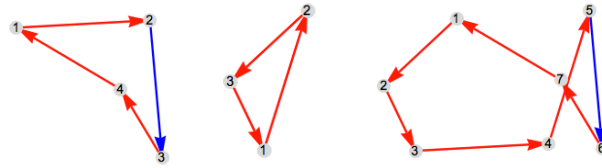

Figure 9: Minkowski sum of two virtual polygons, in the colored polygon representation.

Minkowski inverses. The above operations turn the three sets of objects into groups, since all the elements are invertible (Figure 10).

1. In the star representation, the inverse is obtained by reversing the color and orientation of all star segments.

2. In the balanced weighted unit vector representation, each weight w_i is replaced by its negation $-w_i$.

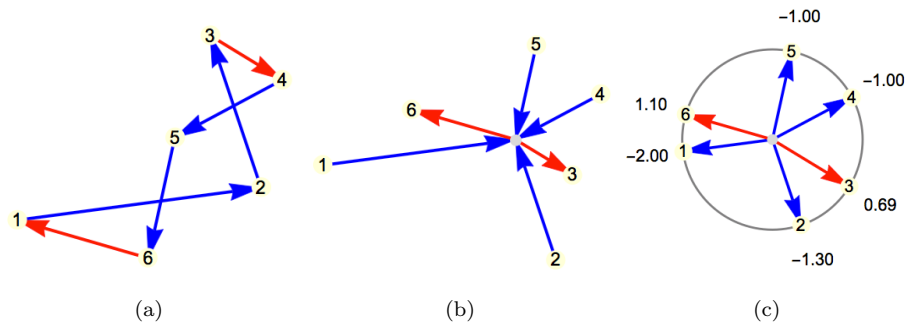3. The inverse of a virtual polygon is a rotation by π of the original polygon with inverted colors.

Figure 10: The Minkowski inverse of the virtual polygon from Figure 6, in each of the three representations: (a) colored poygon, (b) colored star and (c) weighted units.

We summarize the previously described constructions as:

Theorem 3. *The groups of colored polygons, colored stars and weighted units are pairwise isomorphic, and the isomorphisms arise from the direct conversions*

described above. All three groups are canonically isomorphic with the group of 2D virtual polytopes.

Proof. The semigroup of 2D convex polytopes embeds in all the three groups via the *red star* representation of convex polygons. Each group is generated by the image of this inclusion, since each colored star is a difference of two red stars. □

Faces of a 2D virtual polytope represented by a colored polygon. A 2D virtual polytope K represented by a colored polygonal chain $(p_1, ..., p_k)$ has three types of faces, ranked by dimension. The 0-faces are the points $\{p_1, ..., p_k\}$ and the (unique) 2-face is the polytope K itself. The 1-faces are colored segments of two types, red and blue, as discussed in this section. Red edges represent 1-dimensional (convex) segments, whereas blue ones represent inverses to convex segments, as was discussed in Section 2.

3.4   Examples of virtual polygons

To help develop intuitions about distinguishing properties of virtual polygons, we present now a collection of illustrative examples.

Example 1. (Minkowski inverse of a convex polygon) *Since the inverse of a star reorients the edge vectors, the inverse of a convex polygon is a rotation by π of the original polygon with all edges colored blue.*
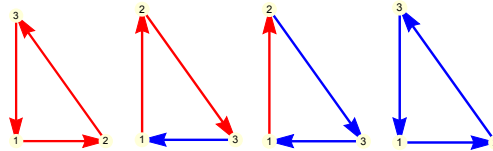

Figure 11:   All the 8 possible colorings of a triangle are virtual polygons (only 4 are shown). This example illustrates how colors differentiate convex and virtual polygons. The edge orientations are induced by the corresponding colored stars.

Example 2. (Colorings of convex polygons) *All of the 8 colorings of a triangles (of which, 4 representatives are shown in Figure 11) are virtual polygons. Only 4 of the colorings of a quadrilateral (Figure 12) are virtual polygons.*

Example 3. (Six-gon and Double covered triangle) *The double-covered triangle from Figure 13 (right) arises by applying the* star-to-polygon *procedure to the shown colored star. This illustrates the fact that virtual polygons, as opposed to convex polygons, may not be simple. They may also have pairs of edges with parallel directions, but, in the star, these have to go in opposite directions.*
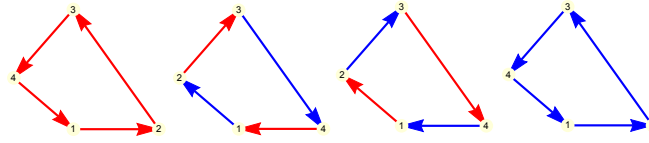
17

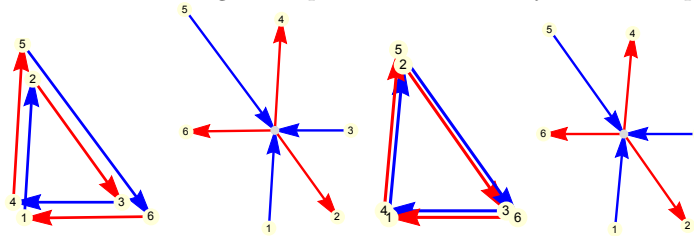Figure 12: The 4 colorings of a quadrilateral which yield virtual polygons.

Figure 13: Left, a virtual 6-gon with parallel pairs of edges and its star. Right, an extreme situation, where the 6-gon becomes a double-covered triangle and the star has pairs of equal but complementary colored vectors.

Example 4. (Aligned edges) *The examples in Figure 14 further illustrate that virtual polygon edges may have the same slope, even with overlap. In Figure 14(left), the aligned edges have the same color, and they overlap in the polygon. In Figure 14(right), they have different colors, and are aligned but do not overlap in the polygon.*
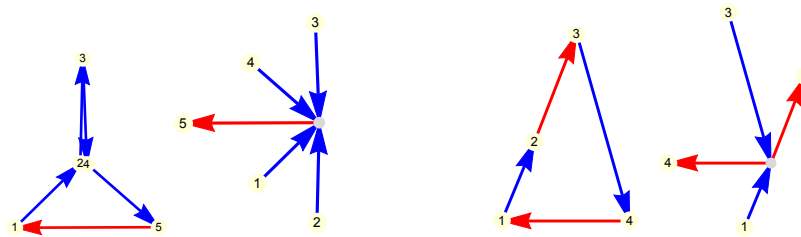

Figure 14: Left, alignment of two oppositely oriented edges with the same color (shown slightly apart for clarity). Right, alignment of two similarly oriented edges with opposite colors.

Example 5. (Multiple self-intersections) *Virtual polygons can have multiple self-intersections, as illustrated in Figure 15.*

3.5 Uncolored virtual polygons

We have so far described representations of 2D virtual polytopes as colored polygons with certain specific properties. It is natural to ask whether being
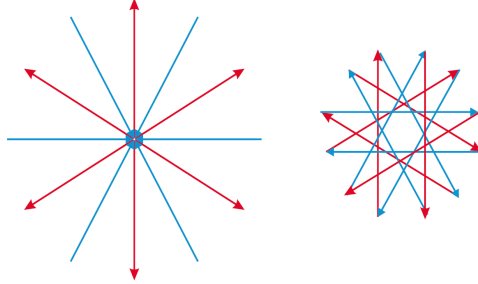
Figure 15: Minkowski difference of two regular hexagons.

"virtual" may be just a property of the polygon (and not of the polygon with the extra colors on edges). If that would be the case, then we could forget the colors in the representation, and reconstruct them when needed. However, we show in this section that the *color forgetting mapping* from virtual polygons to polygons is neither surjective nor injective.

Definition 4. *A polygon with the property that it admits a coloring as a virtual polygon is called a* v-polygon.

Example 6. (Not all polygons are v-polygons) *The two examples in Figure 16 are not v-polygons. In the first example, the existence of groups of more than two parallel edges is an immediate indicator that this is not a virtual polygon, since no matter how we will orient them, there will always be more than one edge vector with the same defining angle. For the second example, we try to find a good coloring, but we will fail because the edge vectors will jump all over the place instead of allowing a consecutive, naturally ordered placement.*

This example suggests the question to *recognize which polygons admit virtual polygon colorings.* An inefficient solution is to list one by one all the 2^n possible colorings on the edges and to keep only those that yield properly ordered colored stars. However, we can show that there exists a simple, linear time algorithmic solution to this problem.

The examples in this subsection clarify the role of colors. We have already seen in the examples from Figure 11 and Figure 12 that some polygons may have no good coloring that would make them virtual polygons, while others may have several. The second question addressed here is that of deciding if a given polygon has or does not have a virtual 2D polytope coloring.

Definition 5. (Ambiguous v-polygon) *A v-polygon that admits multiple virtual polygon colorings will be called* ambiguous.
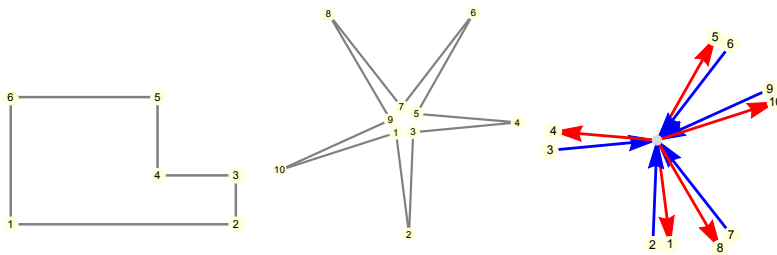
19

Figure 16:   Two polygons which do not admit colorings as virtual polygons. (Left) This polygon has more than two parallel edges. (Middle) A polygon on which any attempt at producing a coloring would fail. (Right) A partial coloring of the first 8 edges cannot be extended to a complete virtual polygon coloring.

Example 7. (There exist ambiguous v-polygons) *The triangle from Figure 11 and the rectangle from Figure 12 have several, distinct colorings. Thus these polygons do not allow for unique reconstruction of the colors of a virtual polygon.*

Remark. The colorings of a v-polygon always come in pairs: whenever we have a coloring yielding a virtual polytope K, the inverse coloring yields the virtual polytope which is Minkowski inverse to the symmetric image of K.

4 Virtual polytopes in arbitrary dimension

We turn now to four representations for virtual polytopes which are possible in all dimensions. For each one we describe a group of geometric objects which is shown to be canonically isomorphic to the group of virtual polytopes. Each section follows this pattern: (a) we first describe a set of geometrical objects together with a group operation; (b) we then show that the semigroup of convex polytopes embeds in this group, and finally (c) we show that the group is generated by the convex polytopes. Direct isomorphisms between some of these pairs of representations are also illustrated in some cases.

4.1 The algebra of polytopal functions

Virtual polytopes appear in the *algebra of polytopal functions* defined by A. Khovanskii and A. Pukhlikov [19], with motivations coming from the algebraic geometry of toric varieties. This last aspect will be discussed in Section 6.5. To gain intuitions, we compare virtual polytopes in 2D represented by colored polygons with the polytopal functions introduced in this section. We also note that this representation has a natural isomorphism from the combinatorial Picard group representation described later in Section 4.4.

Characteristic functions of convex polytopes. We build the algebra starting from characteristic functions of convex polytopes:

$$I_K : \mathbb{R}^n \to \mathbb{R}$$

defined by

$$I_K(x) = \left\{ \begin{array}{ll} 1, & \text{if } x \in K \\ 0, & \text{otherwise.} \end{array} \right.$$

Polytopal functions. A *polytopal function* is a function $f : \mathbb{R}^n \to \mathbb{R}$ which is representable as a finite linear combination $f = \sum \alpha_i I_{K_i}$ of characteristic functions of convex polytopes K_i. The coefficients α_i (called *weights*) are arbitrary integer numbers, possibly negative. The summands I_{K_i} may come from convex "pieces" of different dimensions, including points.

We emphasize that in the construction of the algebra of polytopal functions *translations are not factored out,* that is, two polytopes that differ on a translation are considered to be different.

Such a representation of a polytopal function is never unique, as illustrated in Figure 17. Here, the (characteristic function of) the rectangle is expressed as *"rectangle plus rectangle minus segment",* or as *"triangle plus triangle minus diagonal segment".*
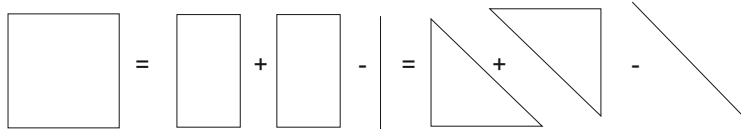

Figure 17: A polytopal function always has infinitely many decompositions.

Ring structure. The set of polytopal functions has a ring structure, induced by the operations of *addition*, defined pointwise, and of *multiplication*, which extends the Minkowski addition $\otimes$ as follows.

Multiplication of polytopal functions. The product $f \otimes g$ of two polytopal functions $f = \sum_i \alpha_i I_{K_i}$ and $g = \sum_j \beta_j I_{L_j}$, is defined as:

$$f \otimes g = \left(\sum_i \alpha_i I_{K_i} \right) \otimes \left(\sum_j \beta_j I_{L_j} \right) := \sum_{i,j} \alpha_i \beta_j I_{K_i \otimes L_j} \tag{1}$$

21

A proof is needed to guarantee that *multiplication is defined correctly*, that is, that the above definition does not depend on any particular representations of the summands. The proof of correctness [19] is based on an equivalent definition of the product of two polytopal functions f, g as the convolution with respect to the Euler characteristic χ:

$$(f \otimes g)(x) = \int_{\mathbb{R}^n} f(x - y)g(y)d\chi(y)$$

Integration and convolution against Euler characteristic is an elegant technique, first defined by O.Viro. The idea of this notion is that the Euler characteristic χ, being an additive function, in some sense resembles a measure. Therefore, in some particular cases one can integrate piecewise constant functions against χ. Since this technique will not be referred to again in this paper, we do not go into further details, which can be found in [47].

The two operations of addition and multiplication turn the set of polytopal functions into a commutative ring, with the identically-zero function as its zero element, and I_E as the unit element, where $E = \{0\}$ is the one-point polytope containing the origin. We focus in this paper on the ring structure, although polytopal functions constitute an algebra over rational numbers.

Convex polytopes are invertible. A remarkable property of the convex polytopes is that their characteristic functions are invertible in this ring.

We start with an auxiliary construction. Let K be a convex polytope. The interior of K taken in its affine hull is called its *relative interior* and is denoted by $Rint(K)$. The central symmetry with respect to the origin O is denoted by $Symm$.

It is not hard to show that the characteristic function of the relative interior of a convex polytope K:

$$I_{Rint(K)}(x) = \left\{ \begin{array}{ll} 1, & \text{if } x \in Rint(K); \\ 0, & \text{otherwise.} \end{array} \right.$$

is a polytopal function.

Theorem 4. *[19] For any convex polytope K, the function I_K is invertible in the ring of polytopal functions. The inverse is expressed as:*

$$(I_K)^{\otimes -1}(x) = (-1)^{dimK} I_{Rint(Symm\ K)} = \left\{ \begin{array}{ll} (-1)^{dimK}, & \text{if } x \in Rint(Symm\ K); \\ 0, & \text{otherwise.} \end{array} \right.$$

Corollary 5. *[19] The algebra of polytopal functions contains a multiplicative subgroup which, after factorization by translations, is isomorphic to the group of virtual polytopes. The isomorphism maps each convex polytope K to its characteristic function I_K. The mapping extends to the entire group, that is, the*

Minkowski inverse $K^{\otimes -1}$ is mapped to the polytopal function described above in Theorem 4.

Now it makes sense to speak of *virtual polytopes represented by polytopal functions.* In the paper of A. Khovanskii and A. Pukhlikov [19] it is shown that virtual polytopes almost exhaust all invertible polytopal functions:

Theorem 6. *[19] Every invertible element of the ring of polytopal functions is, up to a sign, a virtual polytope. More precisely, for any invertible polytopal function f, either f or $-f$ is a virtual polytope.*

An invertible polytopal function $f = \sum_i \alpha_i I_{K_i}$ represents a virtual polytope iff $\sum_i \alpha_i = 1$.

A necessary and sufficient condition for a polytopal function to be invertible appeared in the same paper [19].
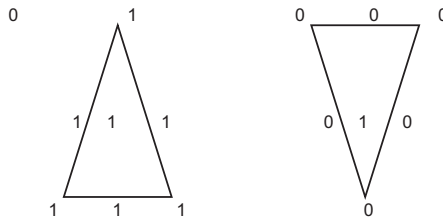

Figure 18: (Left) Polytopal function representing a convex triangle and (Right) its inverse.

Examples. To build the intuition, we illustrate with virtual polytopes represented by polytopal functions in dimension two. Since such functions are piecewise constant, the figures mark the domains by the values of the function. Figure 18 (b) depicts a function which is identically 1 strictly inside the triangle and identically zero outside the triangle and on its boundary. Figure 19 depicts a function which equals -2 inside the triangle, -1 on the boundary, and is zero outside.

Figure 20 illustrates the multiplication of polytopal functions according to the definition. The goal is to compute the Minkowski sum of the convex triangle and the negatively weighted open segment.

First we express the negatively weighted open segment as *"endpoint plus endpoint minus the (closed convex) segment"*. Next, we open the brackets and perform classical Minkowski addition. This gives us two triangles and one negatively weighted trapezoid. We depict them separately, but actually they overlap. Finally, one has to sum up the weights. This gives us the last figure. As we see soon, the negatively weighted open segment represents the Minkowski inverse of the convex segment. So the result of this computation is a virtual polytope,
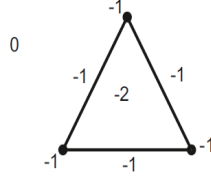
Figure 19: The double covered virtual triangle from Figure 13 represented as a polytopal function.

namely, the Minkowski difference of the triangle and the (convex) segment represented by a polytopal function.

For a comparison of the two representations for virtual polygons (as colored polygons and as polytopal functions) we point to the three examples in Figures 18, 19 and 21. Figure 18 shows a convex triangle and its inverse, which in the colored polygon representation would have the opposite color. Figure 19 represents the double covered virtual triangle from Figure 13. Figure 21 represents the virtual polygon from Figure 6 by a polygonal function.

Historical Note. The polytopal algebra has been defined by A. Khovanskii and A. Pukhlikov in [19], although many ideas can be traced back to Grömer [14]. However, they used a different terminology (*convex chain*), which we have not adopted here because of the potential of confusion with other terminology used in this survey. The alternative name of *polytopal functions* was used in Panina [32, 33]. We restricted our presentation to the ring structure of this algebra, since the structure of the $\mathbb{Q}$-algebra (whose details appear in [19]) although important, is irrelevant for the purposes of this survey.

4.2   McMullen's polytope algebra

We turn now to a second representation for virtual polytopes, Peter McMullen's polytope algebra Π [26]. It is closely related, yet not identical to the Khovanskii and Pukhlikov algebra of polytopal functions defined in the previous section. A crucial difference is that now the translations are factored out, and this has important algebraic consequences. In particular, it implies the existence of a lot of nilpotent elements, which in turn lead to a lot of invertible elements. By contrast, there are no nilpotent elements in the algebra of polytopal functions.

The group of virtual polytopes $\mathcal{P}^*$ appears here in a completely different way, and it is not isomorphic to the (multiplicative) group of invertible elements. As shown below, $\mathcal{P}^*$ is isomorphic to an additive group of the polytope algebra Π
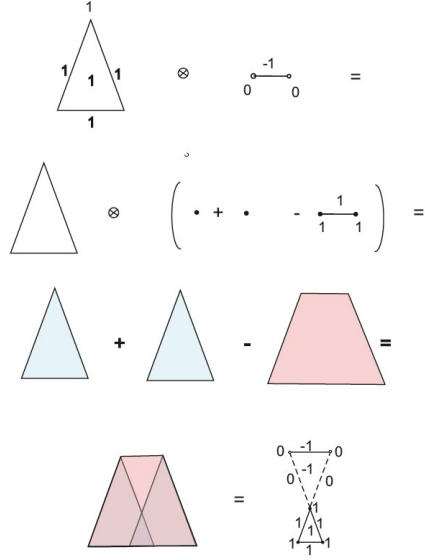
Figure 20: An example illustrating multiplication in the algebra of polytopal functions.

called the *first weight space.*

Definition 6. *(McMullen's Polytope Algebra [26])*

The polytope algebra $(\Pi, +, \otimes)$ *is defined over the set of symbols* $[K]$, *where* K *ranges over the set of all convex polytopes in* $\mathbb{R}^d$. *Additive expressions are subject to the equivalence relations:*

$$[K] + [L] \quad = [K \cap L] + [K \cup L] \quad \text{when } K, L \text{ and } K \cup L \text{ are convex} \quad (2)$$

$$[K] \quad = [K + t] \quad \text{when } K \text{ convex, and } t \text{ a translation vector} \quad (3)$$

Multiplication is first defined for convex polytopes K, L *via Minkowski addition* $[K] \otimes [L] := [K \otimes L]$, *and then extended by linearity to all elements of* Π.

Multiplication by rational numbers in the polytope algebra does not always exist. But in the case when it exists, it can be defined in a unique way. Indeed, multiplication by an integer number reduces to taking a finite sum, which is already defined. Division by an integer requires more care.

Proposition 7. *[26] For any element of the polytope algebra* $\sum \alpha_i[K_i]$ *and any non-zero integer* a *such that* $\sum \alpha_i$ *is dividable by* a, *there exists a unique*
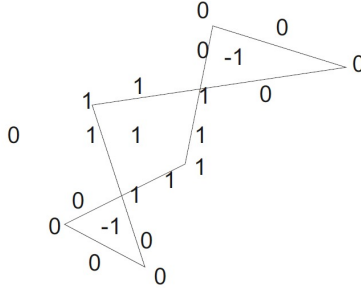
25

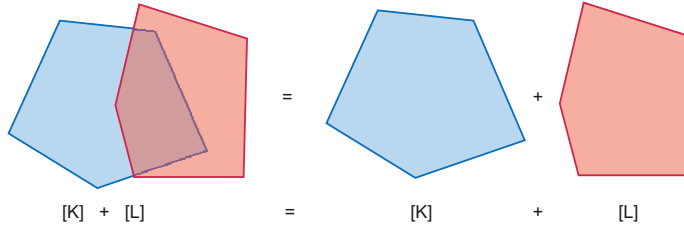Figure 21: Virtual polygon from Fig. 4 represented as a polytopal function.

Figure 22: In McMullen's algebra, the convex polytopes are taken up to translation. These two objects are identified.

element of the polytope algebra f such that $af = \sum \alpha_i[K_i]$. This enables us to write $f = \frac{1}{a} \sum \alpha_i[K_i]$. If $\sum \alpha_i$ is not divisible by a, then such an f does not exist.

Thus, the elements of the algebra are linear combinations with integer coefficients of the form $\sum \alpha_i[K_i]$, subject to the equivalence relations (2) and (3). Fig. 22 and 23 provide illustrations. The unit element E is the one-point polytope, which is very similar to the algebra of polytopal functions.

This construction automatically comes with a canonical surjective homeomorphism from the algebra of polytopal functions to McMullen's polytope algebra Π.

Although McMullen's polytope algebra Π looks very similar to the algebra of polytopal functions, its group of units (invertible elements under multiplication) is much bigger than the group of virtual polytopes. The reason for this is that if $\Sigma a_i = 0$, then $f = \Sigma a_i[K_i]$ is a nilpotent element, and therefore, $1 - f$ is invertible. The inverse $(1 - f)^{-1} = 1 + f + f^2 + \cdots$ is well defined since the sum is finite in this case. This fact implies almost immediately that an element $\Sigma a_i[K_i]$ in McMullen's polytope algebra is invertible iff $\Sigma a_i = \pm 1$.
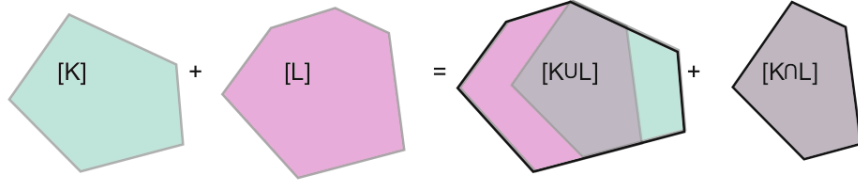
Figure 23: This illustrates the generating relations in McMullen's algebra.

Weight spaces. McMullen's algebra Π has the structure of an (almost) graded algebra, i.e. it is decomposable into a direct sum of graded components, called *weight spaces*. This decomposition has a deep interpretation in terms of the Chow rings associated to toric varieties, and will be briefly discussed in Section 6.5. The other details, although very interesting, are not relevant for our discussion, and can be found in [26].

The decomposition of Π into the sum of graded components is very similar to the graded decomposition of the algebra of polynomials. With this analogy in mind, the k-th graded component consists of homogeneous polynomials of degree k. The latter can be recognized using dilation, since they are exactly those polynomials that satisfy $p(\lambda x) \equiv \lambda^k p(x)$ for every real λ. Analogously, an element f in the polytope algebra is *degree one homogeneous* if, for every positive integer λ, the dilation by λ (which we denote by $(\lambda)f$) coincides with the sum of λ copies of f:

$$(\lambda)f = \underbrace{f + ... + f}_{\lambda}.$$

It is worth mentioning that a convex polytope is not homogeneous in this respect.

Definition 7. *The first weight space of Π is defined as the set of homogeneous elements of degree one.*

The first weight space is clearly an additive group.

Example: homogeneous element in dimension one. If K is a segment and P is a point, then $[K] - [P]$ is homogeneous of degree one, and therefore belongs to the first weight space.

Theorem 8. *([28], Lemma 2.2) The group of virtual polytopes is isomorphic to the first weight space of McMullen's polytope algebra.*

The isomorphism sends a convex polytope K to

$$log(K) = \sum_{i=0}^{\infty} (-1)^{i+1} \frac{([K] - E)^i}{i},$$

27

where E is the one-point polytope, i.e. the unit element in Π.

Since $[K] - E$ is a nilpotent element, the above sum is finite.

It will be seen in Section 6.5 that this theorem relates the Picard group of a toric variety to the group of virtual polytopes.

Historical Note. The definition of the polytope algebra was motivated by the *scissors congruence problem*, which in turn originated from Hilbert's Third Problem. The group of all (isometrical) motions of the space used in the classical setting is replaced here by translations. This allows to introduce multiplication, which would otherwise be impossible. The algebra can be viewed as the universal group for translation-invariant finitely additive measures on polytopes, called *translation-invariant valuations*, and therefore fits into the theory of valuations. The polytope algebra has several remarkable isomorphic interpretations. One is the direct limit of Chow rings of toric varieties [13], the other is via piecewise polynomial functions with respect to some fan [6].

The most remarkable about McMullen's algebra is its relationship to the *g-theorem* that characterizes the face-vectors of simple polytopes. The necessary and sufficient conditions were conjectured in 1970 by P. McMullen. The first proof of the necessity part by R. Stanley used an approach from algebraic geometry, and holds only for rational polytopes, since only those yield algebraic toric varieties. Later on, P. McMullen [27] proved the necessity part for all simple polytopes, using the weight space decomposition in the polytope algebra.

Convex polytopes yield another interesting algebraic structure, the *ring of simple polytopes*, see [8], [9]. However, that does not contain the group of virtual polytopes.

4.3   Support functions

Support functions of smooth convex polytopes represent a well-established concept in convex geometry. Since they behave additively with respect to Minkowski summation, the subtraction of support functions is expected to correspond to Minkowski difference. Just like convex polytopes, the virtual polytopes have piecewise linear support functions and outer normal fans. The convexity property of the support function and of the fan is however relaxed, but all the other properties are maintained.

Cones, fans and spherical fans. The definition of support functions implies cones and fans, so we first introduce these concepts. A *cone* $\sigma \subset \mathbb{R}^n$ is a closed set of points such that for any $x \in \sigma$ and any non-negative λ, the point λx lies in σ. Most of the books on convex polytopes, e.g. [12] assume that a cone is convex, since this is the case in the context of convex polytope theory. For our

purposes, we will have to relax this assumptions, hence our cones may not be convex.

We work with *polyhedral cones*, i.e. those having a piecewise linear boundary. The entire space $\mathbb{R}^n$ and the set containing just the origin $\{O\}$ are special cases of cones. A *fan* Σ is a finite collection of polyhedral cones in $\mathbb{R}^n$ such that: (a) any face of a cone $\sigma \in \Sigma$ belongs to Σ, (b) for any two cones σ_1, $\sigma_2 \in \Sigma$, the intersection $\sigma_1 \cap \sigma_2$ is a face of both σ_1 and σ_2, and (c) the union of all the cones equals $\mathbb{R}^n$. A *convex fan* consists only of convex cones.

For a more intuitive visualization, we also introduce the *spherical fan*, which is the intersection of the (standard unit) sphere with the fan. This yields a tiling of the sphere into spherical polytopes (which may be non-convex). Each spherical fan extends to a fan, so we have an easy direct correspondence between these concepts.
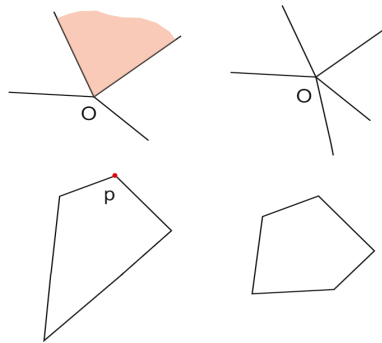

Figure 24: Two convex polytopes together with their fans, illustrated in 2D. On the left, the marked cone in the top figure corresponds to the marked vertex below. The second fan is a refinement of the first one.

A fan Σ is said to be *coarser* than a fan Σ', or equivalently, Σ' is called a *refinement* of Σ, if $\sigma \in \Sigma'$ implies that there exists a cone $\tau \in \Sigma$ such that $\sigma \subseteq \tau$. An example is given in Figure 24.

The *support function* of a convex polytope K is the function

$$h_K : \mathbb{R}^n \to \mathbb{R}$$

defined by

$$h_K(x) = max_{y \in K} \langle x, y \rangle$$

where $\langle x, y \rangle$ is the standard scalar product.

For a generic x, the maximum of the scalar product $\langle x, \cdot \rangle$ is always achieved at one of the vertices of the polytope. For the example in Figure 24, if x lies in

the shadowed cone, the maximum is attained at vertex p. Consequently, on the shadowed cone the support function coincides with the support function of the point p, which is the linear function $\langle p, x \rangle$. Fig. 25 gives an example.

A few well-known properties of the support functions of convex polytopes are summarized in the following lemma.

Lemma 9. *Let K, L be convex polytopes. Let $K + t$ be the translation of K by a vector t. Then:*

- *h_K is a convex continuous piecewise linear function.*

- *The support functions h_K and h_{K+t} differ on a (globally) linear summand.*

- *h_K is positively homogeneous: $h_K(\lambda x) = \lambda h_K(x)$, for $\lambda \geq 0$. In particular, this implies that h_K equals zero at the origin O.*

- *The support function of Minkowski sum equals the sum of support functions:*
$$h_{K \otimes L} = h_K + h_L.$$

Outer normal fan of a convex polytope. There are two equivalent ways to define the fan of a convex polytopes.

- Given a convex polytope K, the linearity domains of its support function h_K yield a fan Σ_K, called the *outer normal fan of the polytope K*, or the *fan of the polytope K* for short.

- Alternatively, the fan of a convex polytope can be defined as follows. For each face F of K, define a cone
$$\sigma_F := \{ v \in \mathbb{R}^n : \ K^v = F \}$$
consisting of those vectors v that the face K^v equals F. The closures of all these cones when F ranges over all proper faces of K is the fan of the polytope K.

An example is illustrated in Fig. 24. We use the second version for defining below the fan of a virtual polytope. The definition implies immediately the following duality property:

Lemma 10. *The faces of a convex polytope K are in a bijection with the cones of a fan Σ_K such that:*

- *A k-dimensional face of K corresponds to a $(n-k)$-dimensional cone of Σ_K.*

- *The affine hulls of a face and the corresponding cone are orthogonal.*

- *This correspondence reverses inclusion.*

Example. Figure 25 depicts a planar convex pentagon, its fan, and the (graph of) the support function.

Remark. In 2D, the spherical fan is obtained from the weighted units representation by a cw rotation by $\pi/2$ followed by forgetting the weights.
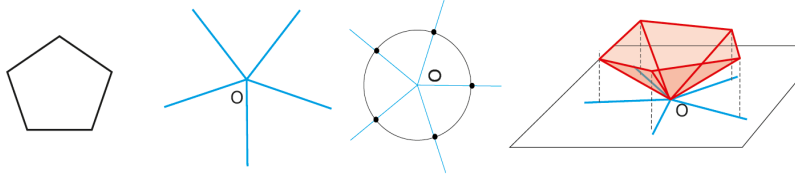

Figure 25: A convex pentagon, its outer normal fan, its spherical fan, and the graph of its support function.

The group of support functions. We consider now the set of all convex continuous homogeneous piecewise linear functions defined on $\mathbb{R}^n$. Each of them is the support function of some uniquely defined convex polytope. With pointwise addition, this set forms a semigroup. We denote by $\mathcal{S}$ this semigroup factored by globally linear functions. The mapping that maps each polytope K to its support function h_K establishes an isomorphism between the semigroup of polytopes modulo translations $\mathcal{P}$ and the semigroup $\mathcal{S}$.

We extend the semi-group $\mathcal{S}$ to the *group of support functions*, that is the Grothendieck group associated to it. It consists of all continuous homogeneous piecewise linear functions h defined on $\mathbb{R}^n$, modulo globally linear functions. Passing to the Grothendieck group means that we allow subtractions of piecewise linear functions. Consequently, we loose convexity, but all the other properties from Lemma 9 are preserved.

The following definition describes the canonical isomorphism between the group of virtual polytopes and the group of support functions:

Definition 11. *Let $K = L \oplus M^{\otimes -1}$ be a virtual polytope. Let h_L and h_M be the support functions of L and M respectively. The* support function *of K is defined as $h_K =: h_L - h_M$.*

31

Since the group of support functions is generated by convex functions, we have:

Theorem 12. *The group of virtual polytopes and the group of support functions are canonically isomorphic. The isomorphism sends a virtual polytope to its support function.*

Definition 8. *Given a virtual polytope K, each face F of K yields a cone*

$$\sigma_F := \{v \in R^n : K^v = F\}$$

consisting of those vectors v that the face K^v equals F. The closures of all these cones when F ranges over all proper faces of K is the fan of the polytope K.

In contrast to the convex case, the cones of the fan may not necessarily be convex. Examples appear in Figures 26 and 27.
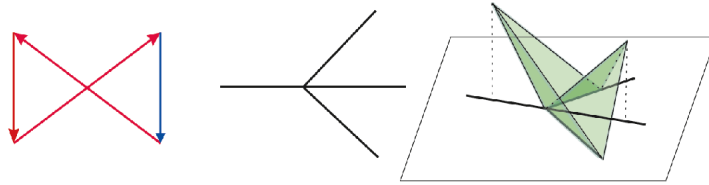

Figure 26: (Left) A virtual polytope represented by a colored chain (middle), its fan (right), and the graph of its support function. In this particular case, the fan is convex, but the support function is not convex.

Figure 27: A virtual polytope represented by a colored chain (left), its fan (middle), the graph of its support function (right). In this particular case, the fan is not convex.

Given a virtual polytope K, the cones of maximal dimension of the fan correspond to vertices of K. This yields a simple, yet important fact:

Lemma 13. *A virtual polytope K is uniquely determined by its fan, vertex set, and the (duality) mapping between vertices of K and the cones of Σ_K of maximal dimension.*

32

Proof. Indeed, we retrieve the support function $h_K(x)$ as the piecewise linear function whose restriction on each of the cones σ_i equals the scalar product (p_i, x). Here p_i is the vertex that corresponds to the cone σ_i. $\qquad\square$

Example 8. *In 2D, the spherical fan is obtained from the weighted units representation by a cw rotation by $\pi/2$ and forgetting the weights.*

More generally, the fan of the support function for a virtual polytope in 2D is retrieved from the colored chain representation by the following algorithm.

Algorithm: (Fan of a 2D virtual polytope)

1. Represent the virtual polygon P by a colored star.

2. Rotate it clockwise by $\pi/2$.

3. Each (colored) segment gives a ray. The collection of all these rays yield a conical tiling of the plane which is the fan of the virtual polytope P. Take the union of 2-dimensional cones that correspond to one and the same vertex.

We conclude with the list of virtual triangles, shown in Figure 28 simultaneously as polytopal functions and as colored chains, together with their fans.
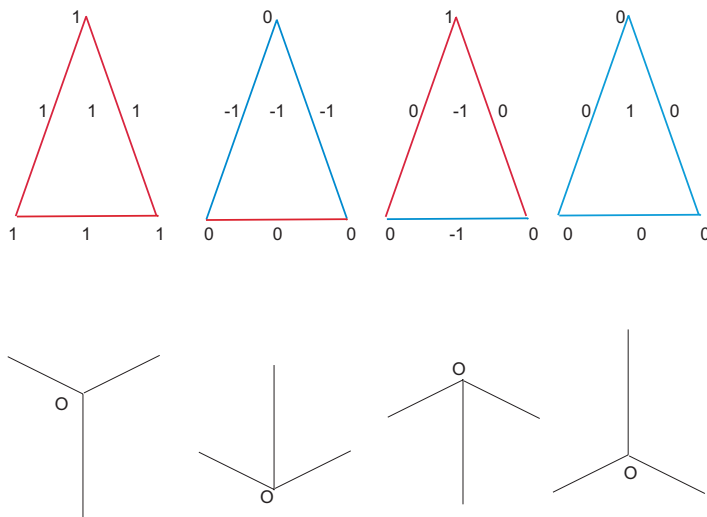

Figure 28: Virtual triangles (represented as polytopal functions and as colored chains), together with their fans.

Historical notes. The idea to pointwise-subtract support functions of convex bodies can be traced back to several sources in the mathematical literature, hence this representation of virtual polytopes may not be a new concept. We

mention in particular an early paper from 1939 of A.D. Alexandrov [1], who considered pointwise differences of support functions when proving a theorem giving a characterization of the sphere. This theorem is the starting point for A.D. Alexandrov's problem discussed in Section 6.1. However, this very terminology and the relevant properties have appeared only recently: the first systematic and explicit study of virtual polytopes defined via their support functions was done in [19], see also [30]. Fans of virtual polytopes appeared (only for 3D) in Rodriguez and Rosenberg [41] and V. Alexandrov [2], but these authors considered only a restricted class of virtual polytopes, called *polyhedral hedgehogs*, which are virtual polytopes with convex fans. These do not cover the entire group of virtual polytopes. Support functions and fans of virtual polytopes were also used by Panina in [34, 33, 35, 37].

4.4 The combinatorial Picard group: systems of translated cones

In this section we introduce the last geometric representation for general virtual polytopes in an arbitrary dimension. It is due to G. Ewald [12]. He explicitly uses the terminology of *virtual polytope* for what we call in this section a *system of translated cones*. There exists a direct correspondence between this representation and the polytopal functions defined previously in Section 4.1.

Dual cone. In this section, all the cones are convex. This is necessary for the definition of the dual cone. Given a convex cone σ, its *dual* cone $\check{\sigma}$ is defined by:

$$\check{\sigma} = \{x \in \mathbb{R}^n : \text{for any } y \in \sigma, \ \langle x, y \rangle \leq 0\}.$$
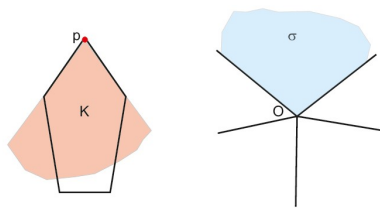

Figure 29: (Left) A cone σ of the fan corresponding to the vertex p_σ of the polygon K. (Right) The translated cone $p_\sigma \otimes \check{\sigma}$.

Translated cones for a convex polytope. Let K be a convex polytope and Σ be its fan. Let a cone $\sigma \in \Sigma$ correspond by duality to a vertex p_σ of K. Then

the cone spanned by K at the vertex p_σ is a translate by p_σ of the dual cone $\check{\sigma}$. In other words, it equals the Minkowki sum $p_\sigma \otimes \check{\sigma}$.

Analogously, if a cone $\sigma \in \Sigma$ corresponds by duality to a face F of K, then the cone spanned by K at the face F is a translate of the cone $\check{\sigma}$ by some p_σ, where p_σ can be choosen to be any point from the affine hull of the face F.

A convex polytope thus naturally yields a system of translated cones. This is illustrated in Figure 29 and Figure 31.

A classical result, known as the *Brianchon-Gram decomposition* [5] (or Gram-Sommerville formula, or Gram's equation), states that the alternating sum of these cones equals the original polytope:

Theorem 14. *[5] Given a convex polytope as a system of cones*

$$K = \{p_\sigma \otimes \check{\sigma}\}_{\sigma \in \Sigma},$$

its characteristic function decomposes in the alternating sum of the characteristic functions of the cones:

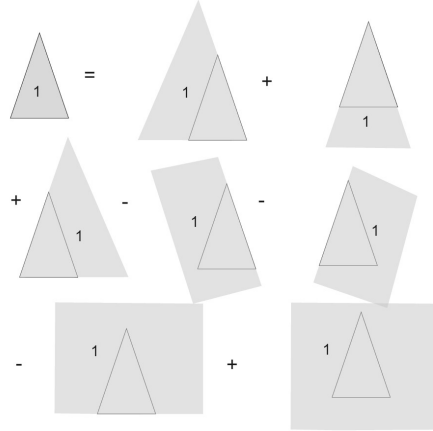$$I_K = \sum_{\sigma \in \Sigma} (-1)^{codim(\sigma)} I_{p_\sigma \otimes \check{\sigma}}.$$

Figure 30: Brianchon-Gram decomposition of a convex triangle.

The following orthogonality property follows directly from Lemma 10.

Lemma 15. *For every cone $\sigma \in \Sigma$, for every one of its faces τ, the vector $p_\sigma - p_\tau$ is orthogonal to the affine span $aff(\tau)$ of the face τ.*

Systems of translated cones.   The previous discussion suggests the following definition:

Definition 9. *Let Σ be a convex fan in $\mathbb{R}^n$ and $\{p_\sigma \in \mathbb{R}^n | \sigma \in \Sigma\}$ be a collection of translation vectors associated to its cones. The collection of translated dual cones*

$$\{p_\sigma \otimes \check{\sigma}\}_{\sigma \in \Sigma}$$

is called a system of translated cones with respect to the fan Σ if the following (consistency) condition holds: for every cone $\sigma \in \Sigma$ and for every one of its faces τ, the vector $p_\sigma - p_\tau$ is orthogonal to the affine span $\mathrm{aff}(\tau)$ of the face τ.

Remark. This definition differs from the notion of the combinatorial Picard group as it was introduced in [12], in that we do not assume that the fan involved is rational, and we do not require that the polytopes involved are lattice polytopes. These conditions appear later, as we pass to toric varieties. But we stress that it is necessary for the fan to be convex, as otherwise duality is not well defined.
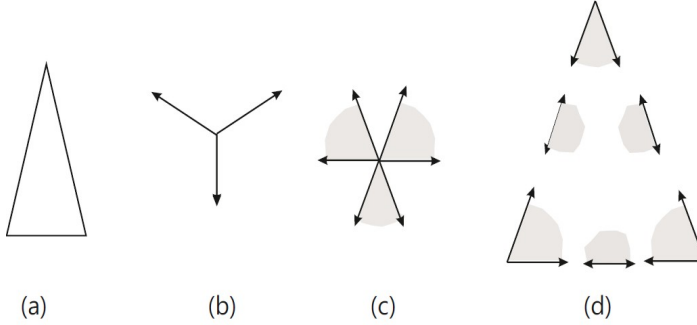
Figure 31:   (a) A triangle, (b) its fan, (c) cones dual to the cones of the fan, (d) translated dual cones.

Group structure on translated cones.   Assuming that a convex fan Σ is fixed, we now endow the system of translated cones with a group structure. The group operation is defined by:

$$\{p_\sigma \otimes \check{\sigma}\}_{\sigma \in \Sigma} + \{p'_\sigma \otimes \check{\sigma}\}_{\sigma \in \Sigma} = \{(p_\sigma + p'_\sigma) \otimes \check{\sigma}\}_{\sigma \in \Sigma}.$$

Since the zero element and the inverse are clearly given by $\{O \otimes \check{\sigma}\}_{\sigma \in \Sigma}$ and $\{(-p_\sigma) \otimes \check{\sigma}\}_{\sigma \in \Sigma}$, we get a commutative group.

Figure 32: System of translated cones for a triangle and its inverse.

To factor out (global) translations, we factorize in the above group by the elements $\{p \otimes \check{\sigma}\}_{\sigma \in \Sigma}$. T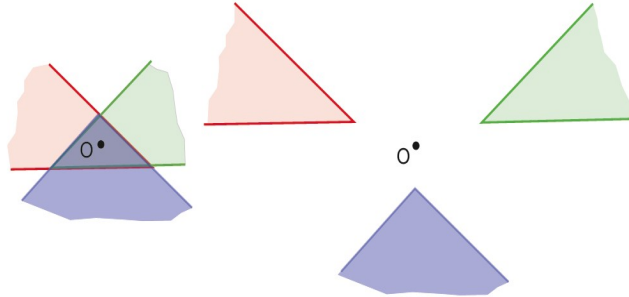hat is, we factor out systems of translated cones with one and the same p for all the cones. After factorization, we get a group $\mathcal{CP}_\Sigma$ which is called (in G.Ewald's book [12]) the *combinatorial Picard group related to the fan* Σ.

The group of virtual polytopes related to a fan.   We are now ready to relate systems of translated cones to virtual polytopes. *The group $\mathcal{P}_\Sigma^*$ of virtual polytopes related to a fan Σ is the subgroup of $\mathcal{P}^*$ consisting of those elements $\mathcal{P}^*$ whose support function is linear on each of the cones Σ. Equivalently, a virtual polytope K is related to the fan Σ, if its fan Σ_K is coarser or equal than the fan Σ.*

The following theorem establishes the canonical isomorphism between the combinatorial Picard group $\mathcal{CP}_\Sigma$ and the above defined subgroup of virtual polytopes.

Theorem 16. *The combinatorial Picard group $\mathcal{CP}_\Sigma$ is isomorphic to the subgroup $\mathcal{P}_\Sigma^*$ of virtual polytopes related to the fan Σ. The isomorphism sends a convex polytope to the associated system of translated cones. Once defined for convex polytopes, it extends to all virtual polytopes.*

Examples.   Figure 32 illustrates two systems of translated cones for a convex triangle and its inverse. The fan of a convex triangle contains 7 cones: three 2-dimensional cones, three one-dimensional cones (rays), and the one-point cone $\{O\}$. Consequently, the dual cones are three pointed cones, three half-planes, and the entire plane (which is dual to $\{O\}$). Figure 31 shows all of them, whereas Figure 32 shows only the pointed dual cones.

From subgroups of virtual polytopes related to a particular fan, we extend now

the definition to the entire group of virtual polytopes. Given a fan Σ and its refinement Σ', we have a natural inclusion $\mathcal{P}_\Sigma^* \to \mathcal{P}_{\Sigma'}^*$. This enables us to speak of *inductive limits* of the groups $\mathcal{P}_\Sigma^*$. This means that we take the union of all the groups and identify the elements using the inclusions defined above.

Theorem 17. *The group of virtual polytopes $\mathcal{P}^*$ is isomorphic to the inductive limit of the groups $\mathcal{CP}_\Sigma$.*

For a virtual polytope, there exists an elegant direct translation from translated cones representation to the representation by a polytopal function. It is a direct generalization of the aforementioned Brianchon-Gram decomposition for convex polytopes:

Theorem 18. *[19] Given a virtual polytope as a system of translated cones*

$$K = \{p_\sigma \otimes \check{\sigma}\}_{\sigma \in \Sigma},$$

its canonical image in the algebra of polytopal functions is the function

$$\sum_{\sigma \in \Sigma} (-1)^{codim \ \sigma} I_{p_\sigma \otimes \check{\sigma}}$$

As an example, this formula can be checked for a triangle using Figure 31.

To summarize, we have presented another equivalent representation of virtual polytopes. This turns out to be the most suitable representation for toric varieties (section 6.5), where a system of translated cones yields immediately an invertible sheaf on a toric variety.

Remark. Analogous constructions are valid if we restrict ourselves to *lattice polytopes*, that is, polytopes whose vertices lie on the standard lattice $\mathbb{Z}^n \subset \mathbb{R}^n$. In this case we obtain the *group of lattice virtual polytopes* $\mathcal{P}_\mathbb{Z}^*$, the *group of lattice virtual polytope related to a fan* $\mathcal{P}_{\mathbb{Z},\Sigma}^*$, and the *combinatorial lattice Picard groups* $\mathcal{CP}_\Sigma^\mathbb{Z}$ and $\mathcal{CP}_\Sigma^\mathbb{Z}$. In this framework it makes sense to consider only rational fans.

Historical Note. The name *"Picard group"* distinctly indicates the original motivation of A. Pukhlikov and A. Khovanskii in connection with the Picard group of toric varieties. This will be briefly sketched in Section 6.5. Ewald in [12] explains in detail the construction of the groups and the relating isomorphisms. It is worth mentioning that the Picard group of a projective toric variety has several equivalent representations: as the group of invertible sheaves, as the group of divisors, and as the group of linear bundles. The translated cones give yet one another representation originating in convex geometry.

5 Virtual 3D polytopes

In the section we give two representations of virtual polytopes which are specific to dimension 3. The goal is to generalize the 2D case, where virtual polytopes appeared as colored *polygons.* In 3D, one would expect some kind of *polyhedral surface.* The first approach represents virtual polytopes as *stressed non-crossing graphs on the sphere.* Simple rules turn the set of spherical stressed graphs into a group, which is shown to be isomorphic to the group of virtual polytopes. The second representation is as a subfamily of *Maxwell polytopes*, called so because these types of polyhedral surfaces appear for the first time in the work of James C. Maxwell. Both geometrizations of 3D virtual polytopes introduced in this section are inspired by, and intimately related to, the theory of planar stressed non-crossing graphs and polyhedral liftings due to Maxwell [24].

Diverse concepts of 3D polytopes appear in the literature: some are non-convex, some have non-convex faces, some are self-intersecting surfaces, some may have non-spherical topology, etc. But the 3D polytopes that we introduce here diverge even further from these familiar examples, in that they may have faces that are not even simple polygons. In our setting, Maxwell polytopes still have vertices, edges and faces. The faces are *flat polygons,* but they need not be simple, i.e. they may self-intersect. The connection to spherical stressed graphs concludes the section.

5.1 Virtual polytopes as stressed spherical graphs

In this section we introduce a distinct representation for 3D virtual polytopes as *stressed non-crossing spherical graphs.*

Non-crossing spherical graphs. A *graph* is a pair $G = (V, E)$, with a finite set $V = \{1, 2, ..., n\}$ of vertices and a finite set E of edges. We allow loops and parallel edges. We also include the *single loop graph*, which is one closed edge with no vertices on it. A graph may contain the single loop graph as a connected component. For technical reasons that will become clear later, we also assume that there are no isolated vertices and no vertices of degree 2.

A *spherical realization* (or *placement*) of the graph is an injective mapping

$$p : V \to S^2$$

of its vertices to the unit sphere S^2, together with a function that maps edges to geodesic segments (great-circle arcs) on the sphere. An edge with endpoints i and j is mapped to a geodesic segment with endpoints at p_i and p_j. The placement is said to be *non-crossing* or an *embedding* if the edge segments do not cross and do not overlap. The edges are not necessarily mapped to the shortest geodesic, so if the vertices of an edge are fixed, there are (at least) two possibilities to place the connecting edge. More precisely, if the edge endpoints

are not mapped to a pair of antipodal points, then there are exactly two possible geodesic arcs that can represent the edge. If the endpoints are antipodal, there is a continuum of possibilities. We also assume that the single loop graph embeds as a great circle (with no vertices).

Such a spherical realization induces a *facial structure* on the graph. Faces are the connected regions (tiles) of the sphere that arise by removing the points and arcs corresponding to the embedding. By construction, the faces are bounded by spherical polygons, but they may not necessarily be topological disks (may have holes). For example, a disconnected graph has at least one non-disk face.
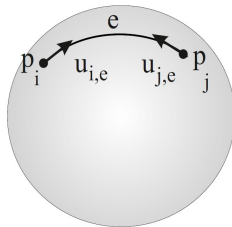

Figure 33: Vectors $u_{i,e}$ used in defining spherical stress.

Stress. Let $N(i)$ denotes the set of edges incident to a vertex $i \in V$. Let $u_{i,e}$ be the unit vector tangent to the geodesic arc corresponding to the edge $e \in E$ at the point p_i, oriented towards the edge, as illustrated in Figure 33. An *equilibrium stress* on a spherical embedded graph is a mapping from the edges to the reals:

$$s : E \to \mathbb{R}$$

which satisfies the *equilibrium condition* at every vertex $i \in V$:

$$\sum_{e \in N(i)} s_e u_{i,e} = 0 \tag{4}$$

By definition, we also assign a stress, which can be any number, on the edge of the single-loop graph.

A stress is *non-trivial* if it is not identically zero. A stress is *non-zero* if it is non-zero on every edge.

Note. This definition is a slight modification of the similar concept used by Maxwell [24] for planar graphs and adjusted here for the sphere. The intuition behind it comes from imagining the edges as springs lying on the sphere. Depending on whether they are stretched or compressed compared to their natural state, the system of springs associated to a graph is in equilibrium exactly when

condition (4) holds. The vector $s_e u_{i,e}$ equals the force applied on the point p_i by the spring along edge e.
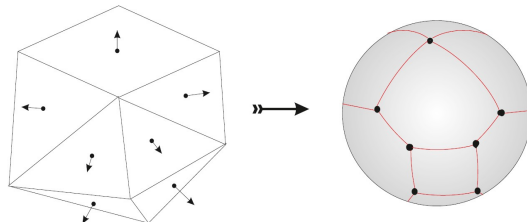

Figure 34:   A convex polytope yields a positively stressed graph.

In drawing such graphs, we color in red the positively stressed edges, that is those with $s(e) > 0$. Negatively stressed edges are colored in blue. The following proposition gives the important correspondence between convex polytopes and stressed spherical graphs.
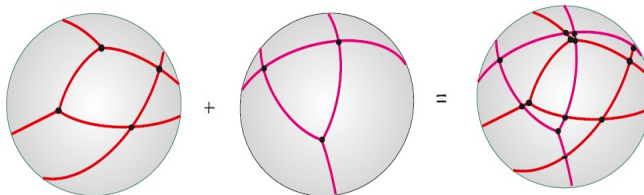
Figure 35:   The sum of two positively stressed graphs.

Proposition 19. *Let $K \subset \mathbb{R}^3$ be a convex polytope. Its spherical fan yields a spherically embedded graph G_K, whose edges correspond (by duality) to edges of the polytope K. Let the function s_K send each edge of G_K to the length of the corresponding edge of K. Then s_K is a positive equilibrium stress of G_K. Conversely, each positively stressed spherical graph uniquely defines a convex polytope $K \subset \mathbb{R}^3$.*

As a consequence, we can view spherical positively stressed graphs as representations of convex 3D polytopes. We include the single-vertex polytope (represented by the empty graph), the two-vertex polytope (the line segment), repre-

sented by a single-loop graph, and all "flat" polytopes (that is, convex polygons), represented by graphs with two antipodal vertices and at least three edges.

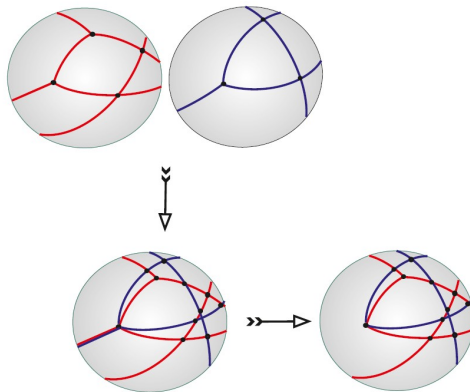Now we turn the set of non-zero stressed graphs into a group.

Figure 36: The sum of two stressed graphs: one is positively stressed, the other one is negatively stressed.

Sum of stressed graphs. The sum of two spherical stressed graphs

$$(G, s) = (G_1, s_1) + (G_2, s_2)$$

is defined via the following algorithm:

Algorithm: (Sum of two stressed spherical graphs)

1. Each of the graphs yields a tiling of the sphere S^2. We take the tiling arising from their common refinement: it may have new vertices, and some of the original edges get split. The 1-skeleton of the common refinement is a spherically embedded graph G.

2. G has a natural stress defined as the sum of s_1 and s_2, as follows. Let $e \in E$ be an edge of G. If it lies on some edge of G_1 and on no edge of G_2, then we assign to e the stress inherited from s_1. If it lies on an edge of G_1 and on an edge of G_2, we take the sum of inherited stresses. The stress obtained is not necessarily non-zero, so we need some further reductions.

3. Remove all zero stressed edges of G. Remove isolated vertices.

4. If vertices of degree two (with two adjacent edges) exist, they must form an angle of π and be equally stressed. In this case, we remove the vertex and collapse its two incident edges into one.

Properties of stressed graphs. The following properties are immediate consequences of the above algorithm: (a) The zero element with respect to addition is the empty graph. (b) The summation of positively stressed graphs corresponds to Minkowski addition of the associated convex polytopes. (c) Each stressed graph has an *inverse*, obtained by simultaneously negating the signs of all its edges. (c) The group of non-zero stressed graphs is generated by the positively stressed graphs.

From this, we obtain immediately:

Theorem 20. *[37] The group of non-zero stressed graphs is canonically isomorphic to the group of virtual polytopes. The canonical isomorphism sends a formal difference of convex polytopes $K_1 \otimes K_2^{\otimes -1}$ to the difference of associated (positively) stressed graphs*

$$(G_1, s_1) - (G_2, s_2)$$

This allows us to speak of *virtual polytopes represented by stressed graphs.*

Historical notes. The material in this section comes from Panina [37]. The advantage of the representation is that it helps to construct virtual polytopes in 3D by just drawing pictures on the sphere. We discuss this in more detail in Section 6.1.

5.2 Virtual polytopes represented by Maxwell polytopes

In this section we turn to a new representation of 3D virtual polytopes as colored *Maxwell polytopes.* They are the closest in spirit to the theory of polytopes, and have not been described as such before. This approach builds upon the intuition developed in dimension two in what concerns non-convexity, self-intersections and the role of the colors.

We define Maxwell polytopes starting from *face graphs*. This purely combinatorial data enables us to speak of combinatorial duality without any reference to geometry. We then show how a virtual polytope can be represented as a colored Maxwell polytope together with an associated fan. We discuss the relevant properties that emerge from this representation and address the problem of detecting which Maxwell polytopes represent virtual polytopes and which do not, as we did in Section 3.5 for colored polygons.

Face graphs and their duals. Recall that *a graph* $G = (V, E)$ is a finite set of vertices $V = \{v_1, \cdots, v_n\}$ and a finite collection of edges E. We allow loops, multiple edges, as well as the single-loop graph, which is one edge with no vertices. In other words, our edges have zero, one or two incident vertices, and the collection of edges is not a set, as it may contain repetitions. To indicate the endpoints of an edge, we write $e = \{v_i, v_j\}$.

A *cycle* $(v_1, e_1, v_2, e_2, \cdots, e_n, v_{n+1})$ of length $n \geq 2$ in such a graph is a circular sequence[12] of vertices and edges, with $v_1 = v_{n+1}$ and $e_i = \{v_{i-1} v_i\}$. Loops with zero or one endpoint are also cycles or length zero, resp. one. A cycle is *simple* if there are no repetitions of vertices, and *edge simple* if there are no edge repetitions.

A **face** is a non-empty set of cycles in the graph G. An edge appearing in the union of all the cycles of the face is said to be incident to the face. We impose the additional constraint that no edge appears more than once in the cycles of a face. In particular, this implies that all cycles of a face are edge-simple.

Definition 10. *A* **face graph** *is a graph G together with a (finite) collection of faces $C_1, ..., C_m$, satisfying the additional property that an edge is incident to at most two faces.*

Intuitively, a face graph captures the combinatorics of a surface. We associate to it a topological space by patching 2D disks (associated to each cycle) along common edges. To a face with $k \geq 2$ cycles we associate a topological sphere with k holes, where each cycle is bounding a disk-like hole on the surface of the sphere. Thus we can associate a topology to each face and, by the glueing rules, to the entire face graph. A (topological) *spherical face graph* is one which topologically is a sphere.

Definition 21. *The dual $G^* = (V^*, E^*, F^*)$ of a non-crossing (topological) spherical face graph $G = (V, E, F)$ has $V^* = F$, $F^* = V$ and $E^* = E$. Two dual vertices (corresponding to two primal faces) are connected by a dual edge whenever the primal faces share an edge.*

The dual of a topological spherical face graph is not necessarily spherical, but it is not hard to describe either: it is a *cactus of spheres*, defined next.

Cactus of spheres. This topological surface is defined inductively. The base case is a topological sphere. At each inductive step, we attach a new sphere at an existing vertex. Underlying the cactus is a tree-like structure, as illustrated in Figure 37. The tree has a node for each sphere and an tree edge between two nodes whose corresponding spheres share a point. The example in Figure 39(left) is obtained by glueing two spheres at a vertex, and is an example of a *cactus* of two spheres.

---

[12]A circular sequence is an ordered list of elements, considered up to circular rotations.
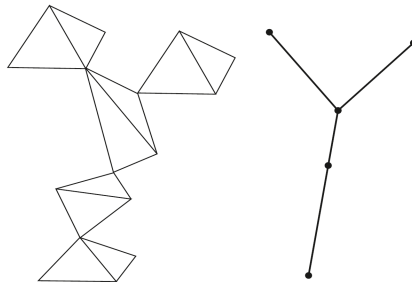
Figure 37: A cactus graph and its underlying tree.

We look now at face graphs arising from stressed graphs on the S^2 sphere.

Embedded spherical graphs. If G is a graph embedded on the sphere, we can define *faces* as being the connected regions of the complement, relative to the sphere's surface, of the union of edge arcs and vertices. The boundary of a face is a collection of cycles in the graph G. If G is a connected graph, then all the faces are disks. Otherwise we obtain faces that are topologically spheres with k holes. The cycles bounding the faces can be consistently oriented, inheriting from a fixed orientation of the sphere. More precisely, we orient them so that a disk-like face lies "on the lefthandside" of its oriented boundary cycle. If the spherical graph is stressed, then its face cycles have no repetitions of edges.

The faces of stressed graphs are related to the spherical fan (see Definition 8) of the corresponding virtual polytope. This motivates us to define the *reduced fan*:

Definition 11. Reduced fan. *Given a 3D virtual polytope K represented by the stressed spherical graph (G, s), its reduced spherical fan is the face graph induced by the embedding of G on the sphere.*

This definition leads to a trivial yet important observation: the faces of the embedded graph are connected components of linearity domains of the support function. With this insight, we discuss now the facial structure of a stressed graph.

A face of a spherical graph G is not necessarily a disk, since the graph may be disconnected, as in Figure 38. Each face of the graph is bounded by a finite collection of disjoint spherical polygons. Therefore, each face is homeomorphic
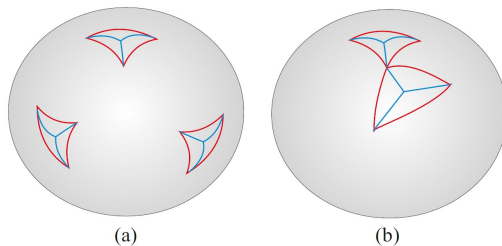
45

Figure 38: (a) Faces of the fan are not necessarily disks. (b) A self-touching face.

to an (open) sphere with holes. A bounding polygon doesn't have crossing or overlapping edges, but it can touch itself vertex-to vertex.

Dual of a spherical face graph. The following properties result from the direct application of the above definitions to the kind of spherical graphs that support a non-zero stress.

1. All the faces of the dual face graph are single cycle sets, and therefore, topological disks.

2. If the graph is connected, its dual is a topological sphere.

3. If the graph has k connected components, then the dual graph has the topology of a *cactus of spheres*.

Maxwell polytopes. With these concepts in place, we turn to one of the main definitions of this section:

Definition 22. *A Maxwell polytope is a face graph together with a (not-necessarily injective) mapping of the vertices to $\mathbb{R}^3$, such that:*

(1) **Non-degeneracy of edges***: The endpoints of each edge are mapped to distinct points.*

(2) **Face planarity condition***: The vertices of each face are mapped to coplanar points. Thus, each face is mapped to a planar (possibly self-intersecting) polygon.*

(3) **Non-degeneracy of faces***: The vertices of each face are not mapped to collinear points. In other words, the image of a face defines a unique plane.*

The images of the vertices, edges and faces of the face graph are called the *vertices, edges* and *faces* of the Maxwell polytope. By the *combinatorics of a Maxwell polytope* we mean the underlying face graph.

46

Virtual polytopes as Maxwell polytopes. Let us consider a virtual polytope K which is neither a segment nor a point. We have seen in Section 2.3 that a virtual polytope has faces which are themselves virtual polytopes of a lower dimension. Thus a 3D virtual polytope K has vertices, edges, and 2D facets.

We make use of the representation of K as the support function h, which comes together with the reduced spherical fan Σ. We also refer to the representation of K as a spherical stressed graph (G, s).

Definition 23. *The Maxwell polytope M associated to the virtual polytope K is defined by an underlying face graph and a placement of vertices.*

(1) The underlying face graph is dual to the reduced spherical fan Σ, or, equivalently, dual to the face graph induced by the stressed graph G.

(2) The placement of vertices first maps each vertex of the dual face graph Σ^* to the corresponding face of Σ, and next, to the corresponding vertex of K.

We now analyze in detail the vertices, edges, and faces of the Maxwell polytope associated with a virtual polytope.

Vertices of the Maxwell polytope induced by a virtual polytope. By duality, a vertex a corresponds to a face of the reduced spherical fan, and therefore, to a domain of linearity of h, which is a cone σ. The restriction of $h(x)$ to the cone σ equals the scalar product $\langle a, x \rangle$. Thus the support function of a virtual polytope can be retrieved from the spherically embedded graph and the vertices of corresponding Maxwell polytope.

Edges of the Maxwell polytope induced by a virtual polytope. By Theorem 1, a vertex of an edge of K is a vertex of K. Therefore, edges of K connect the vertices. Since they are one-dimensional polytopes, that is, virtual segments, we represent them by blue and red segments, as discussed in Section 2. Up to translation, an edge of K corresponding to an edge e of the graph G can be retrieved as follows: if the stress s_e on the edge e is positive, then the edge of K is a convex segment of length s_e which is orthogonal to the affine hull of e. According to our convention, we color it red. If the stress is negative $s_e < 0$, then the corresponding edge of K is the Minkowski inverse to the convex segment of length s_e which is orthogonal to the affine hull of e. This yields a red-blue coloring on the edges.

Remark. A virtual polytopes K and the symmetric image of its inverse $Symm(K^{\otimes -1})$ yield one and the same Maxwell polytope, but with reversed colorings.

Facets of the Maxwell polytope induced by a virtual polytope. Some of the edges form closed planar colored polygons that represent the facets of K. To retrieve the facets and thus the entire Maxwell polytope from the stressed graph representation, we discuss first the case when the graph is connected. In this case, the resulting Maxwell polytope is a topological sphere.

Algorithm 24. Stressed graph to Maxwell polytope (for connected graphs) *Let K be virtual polytope represented by a stressed connected graph (G, s). The associated Maxwell polytope is retrieved as follows:*

1. *Let p_i be a vertex of the graph G, viewed as a unit vector emanating from the center of the sphere. We take the plane π which is orthogonal to p_i. Since it is oriented by the direction p_i, we can to speak of cw and ccw rotations within the plane.*

2. *The star of the vertex p_i induces a colored star in the plane π. Namely, the vectors of the star are the force vectors $s_e u_{i,e}$. The color is assigned in terms of the sign of the stress (red for positive, blue for negative). Since the forces are in equilibrium, the star is balanced.*

3. *The star defines a virtual polygon P represented as a colored polygon (as in Section 3.3) in the plane π.*

4. *After a clockwise rotation of the virtual polygon P by an angle of $\pi/2$, we obtain the face K^{p_i} represented by a colored polygon.*

5. *The above steps retrieve all the faces up to a translation. The combinatorics indicates which should share an edge. We shift the faces by parallel translations as follows: start with one vertex of the graph G and fix a position of the associated face. Take a neighboring vertex in G and its corresponding face. By duality, these two faces share an edge, therefore once the position of the first face is fixed, the position of the second one is determined uniquely. Proceed in this manner taking faces one by one. Since the graph G is connected, we get the positions of all the facets.*

Before considering arbitrary stressed graphs, containing several connected components, we look at one particular example.

Example 9. *A stressed graph with two connected components and its corresponding Maxwell polytope are illustrated in Figure 39. The Maxwell polytope is represented as glueing vertex-to-vertex the two Maxwell polytopes corresponding to the two connected components.*

A disconnected stressed graph (G, s) splits into a disjoint union of its connected components G_i. Each component can be treated as a separate virtual polytope represented by a stressed graph, and therefore gives a Maxwell polytope M_i which is a topological sphere. These polytopes are then glued together vertex-to vertex to form a *cactus* of spherical Maxwell polyhedra.

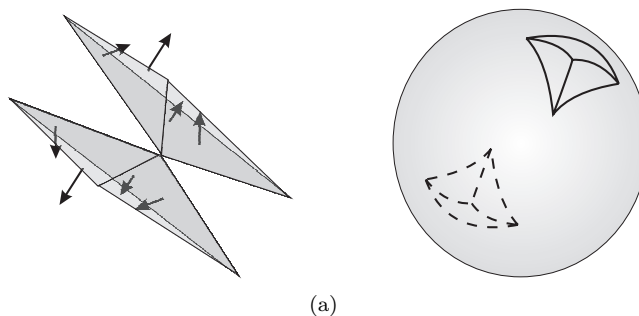These considerations lead to the following algorithm:

(a)

Figure 39: The Maxwell polytope on the left is associated to the non-connected stressed graph on the right.

Algorithm 25. Stressed graph to Maxwell polytope (for disconnected graphs) *Let K be virtual polytope represented by a stressed graph (G, s).*

1. *Decompose G into the union of its connected components G_i. Each connected component comes together with a spherical embedding inherited from G and with the stress inherited from s. For each of the connected components, apply the above algorithm and construct the corresponding Maxwell polytope M_i.*

2. *Each of M_i is recovered up to a translation. Whenever G_i and G_j have edges incident to the same face F of the face graph induced by the embedding of G, the corresponding Maxwell polytopes M_i and M_j should share the vertex that corresponds by duality to F. The Maxwell polytope M is obtained by shifting the M_i's by translations, one by one, in order to be glued in a cactus structure.*

5.3 Detecting virtual polytopes

In this section we consider the problem of detecting which spherical graphs correspond to virtual polytopes. We restrict the discussion to connected face graphs, whose duals are topological spheres. The general case of disconnected follows immediately. We start by analyzing the more structured case of trivalent graphs.

Simplicial virtual polytopes in 3D. Let us consider a 3D virtual polytope K represented by a stressed connected *trivalent* graph (G, s): each vertex of G is incident to exactly three edges. Then each face of the associated Maxwell polytope is a virtual triangle, that is, a triangle with some coloring on the edges. Triangles are patched together edge to edge whenever the corresponding vertices of the graph are connected by an edge. In other words, the Maxwell polytope M that represents K is a *simplicial surface in $\mathbb{R}^3$*. For this reason, we refer

49

to this kind of virtual polytope K as a *simplicial virtual polytope*. A number of simplicial virtual polytopes with particular geometrical and combinatorial properties are illustrated in Example 13, Figure 41 and Figure 48.

Detecting simplicial virtual polytopes in 3D. Let us consider an arbitrary sphere-homeomorphic closed simplicial surface M, given as a collection of (uncolored) triangles patched edge-to-edge in such a way that each edge is shared by exactly two triangles. We do not require M to be embedded or even immersed, thus the surface may have both global and local self-intersections, but we ask that no two adjacent triangles have the same affine hull (that is, they do not lie in the same plane).

As a 3D counterpart of Definition 4 we have:

Definition 26. *A Maxwell polytope is a* v-polytope *if it is associated to a virtual polytope given by a stressed spherical graph.*

Most of the simplicial surfaces are not v-polytopes. The answer to the natural question: *given a simplicial surface M, is it a v-polytope?* is given algorithmically.

Algorithm 27. *[34]* **Is a simplicial surface a v-polytope?**

Let M be a simplicial surface.

1. *Choose a normal vector to each of the (triangular) facets. This can be done independently, that is, we do not require that the collection of all normal vectors yields a global orientation of M. The normal vectors for different facets should be different. If this is not possible, then there is no virtual polytope associated to the surface.*

2. *Mark on the unit sphere S^2 the endpoints of all the normal vectors.*

3. *Whenever two marked points correspond to two adjacent facets of M, connect them by a geodesic arc (an edge). For non-antipodal points, we may choose either the short or the long arc. The result should be an embedded graph, i.e., these edges must not have intersections. If we succeed, we have obtained a spherical fan Σ.*

4. *If no such assignment of normal vectors or no embedded graph can be found, then we conclude that there is no virtual polytope associated with the surface.*

5. *Otherwise, each such fan Σ together with the surface M give a virtual polytope K represented by the pair (M, Σ).*

The surface M was presented with uncolored edges but if an associated virtual polytope exists and is found, then a set of compatible colors will be retrieved

from any stress associated to the fan. Since the stress may not be unique, neither would be the coloring.

Remarks about the algorithm. We emphasize that different fans on the same surface induce different virtual polytopes. The spherical fan Σ is the reduced spherical fan of the virtual polytope K found to be compatible with the given surface M. For a vertex p of the surface M and a face A of the reduced fan Σ which is related to p by duality, the restriction of the support function h_K to the cone A equals the (globally) linear function represented by the scalar product $\langle p, x \rangle$.

Ambiguous v-polytopes. A Maxwell polytope is said to be an *ambiguous v-polytope* if it supports at least two non-complementary virtual polytope colorings. An example is provided by the surface of a tetrahedron, which is very ambiguous: there exist 52 virtual polytopes associated to it, shown in Example 10.

The generic case: non-trivalent stressed graphs. We turn now to the general case. If a virtual polytope P is represented by a non-trivalent stressed graph, then its Maxwell polytope is not a simplicial surface. In fact, it may be not a surface at all, as the polygons representing the faces may have self-intersections. An extension of the previous algorithm can answer the question: *Is a Maxwell polytope a v-polytope?* The algorithm is almost the same, except for an additional case (inserted between steps 3 and 4 of Algorithm 27) needed to treat antipodal points that should be connected by an edge.

Algorithm 28. Is a Maxwell polytope a v-polytope? *Let M be an uncolored Maxwell polytope.*

1. *Choose a normal vector to the plane of each of the facets of M. The normal vectors for different facets should be different. If this is not possible, then there is no virtual polytope associated to the surface.*

2. *Proceed as in Algorithm 27 A necessary addendum is the following:*

   Assume that two antipodal points correspond to two adjacent faces sharing an edge e. These two points also should be connected by an edge, but this time with an extra condition: the connecting arc on the sphere should be orthogonal to the affine hull of e. Again, we can choose between two options: we can take either one or the other semicircle.

3. *If we end up with a fan Σ, then the fan Σ, and the surface M together give a virtual polytope.*

The orthogonality condition that appears here is necessary. It has been discussed 5.2.

Thus we can speak of virtual polytopes represented by a Maxwell polytope M, together with an associated reduced fan Σ.

5.4   Examples of 3D Virtual Polytopes

We present now a collection of virtual polytopes in 3D. They are obtained by presenting a Maxwell polytope which turns out to be a v-polytope, according to Algorithms 27 and 28. The examples present a virtual polytope as a Maxwell polytope and also show its associated fan.
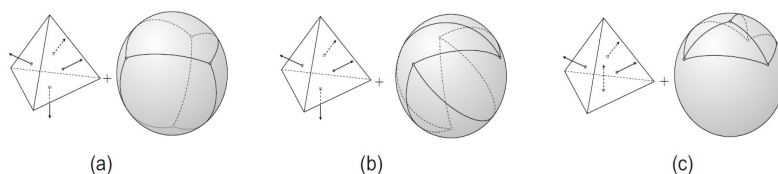

Figure 40: (a) Convex tetrahedron, (b) hyperbolic tetrahedron, (c) yet another virtual tetrahedron associated with the surface of a convex tetrahedron.

Example 10. The tetrahedron is v-ambiguous. *There exist 52 different virtual polytopes associated with the surface of a convex tetrahedron. We depict three of them separately in Figure 40, and give the complete list in Figure 41. The second tetrahedron in Figure 40 represents the family of hyperbolic virtual polytopes, to be defined and discussed in Section 6.1.*

Example 11. A v-polytope with self-intersecting faces. *Figure 42 shows a virtual polytope with self-intersecting faces.*

The vertex-edge graph of a virtual 3D polytope is always connected. A graph is *k-connected* if removal of any $k - 1$ vertices with adjacent edges leaves the graph connected.

Example 12. A v-polytope with two-connected vertex-edge graph. *Balinski's theorem states that the vertex-edge graph of a convex 3D polytope is three-connected, see [48]. We have already seen in Figure 39 that the vertex-edge graph of a virtual polytope can be not two-connected. Figure 43 presents a virtual polytope, whose vertex-edge graph is two-connected, but not three-connected.*

Example 13. A flexible v-polytope. *Cauchy's theorem states that 3D convex polytopes are never flexible: convex polytopes with congruent corresponding faces must be congruent to each other. Unlike convex polytopes, virtual polytopes may*
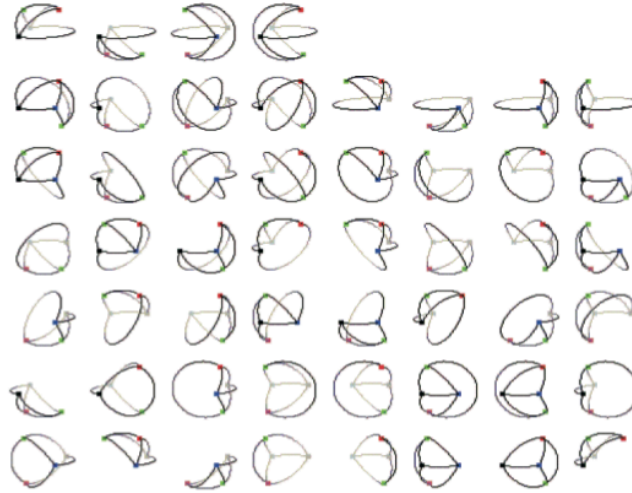
Figure 41: All 52 virtual tetrahedra. We depict here only their fans. (Picture by Vlad Sherbina).
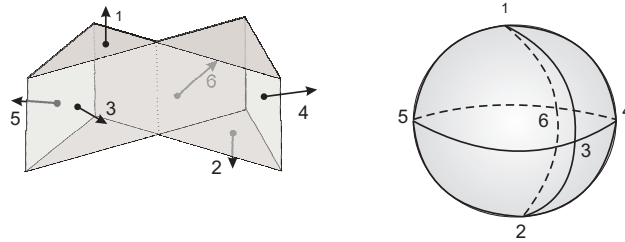

Figure 42: Self-intersecting virtual polytope.

be flexible. Figure 44, left, shows a flexible virtual polytope obtained by using Bricard's flexible octahedron as the Maxwell polytope M, and apply Algorithm 27. The associated fan Σ is depicted in Fig. 44, right.

More sophisticated examples of virtual polytopes will be presented in Section 6.1.

5.5   Support functions and 3D liftings of stressed graphs

The support function representation of a 3D virtual polytope is very closely related to the stressed graph representation and the two can be easily converted into one another.
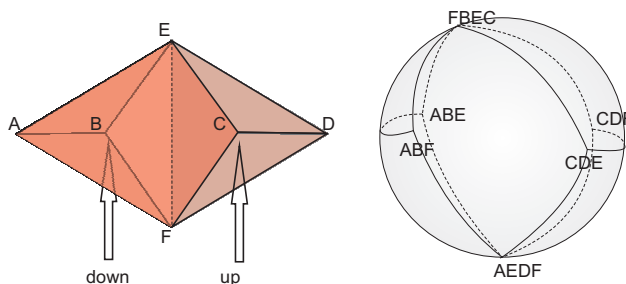
53

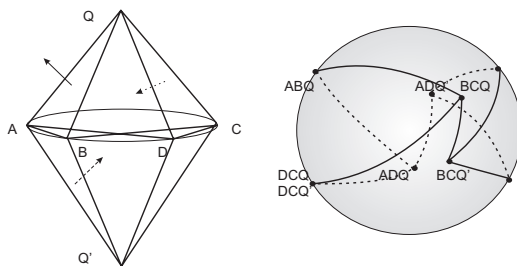Figure 43: Virtual polytope whose vertex-edge graph is not 3-connected.

Figure 44: Bricard's octahedron is a flexible virtual triangulated polytope. Shown here is an octahedron together with the normal vectors of the faces (left) and its fan (right).

We have already mentioned how support function representation relates to the stressed graphs and Maxwell polytopes. For completeness, we give two algorithms that directly relate the stressed graph representation and the support function representation of a virtual polytope.

Algorithm 29. Support function to stressed graph. *Given a virtual polytope K represented by its support function h, the corresponding stressed graph (G, s) is retrieved as follows:*

1. *The linearity domains of h compose the fan associated to K. Being intersected with the unit sphere, the fan yields an embedded graph G. This is the graph we are aiming at; it remains to recover the stress.*

2. *Take an edge e of the graph G. It is incident to two (spherical) polytopes that correspond to two cones, say, σ_1 and σ_2. The two cones share a face $F = \sigma_1 \cap \sigma_2$. By construction, the function h is linear on each of the cones. Let $h = \langle p_1, \cdot \rangle$ on σ_1 and $h = \langle p_2, \cdot \rangle$ on σ_2, where $\langle \cdot, \cdot \rangle$ is the scalar product.*

3. *Set the stress on the edge e equal the scalar product $\langle p_1 - p_2, v \rangle$, where v is the unit outer normal vector to the face F of the cone σ_1 (see Fig. 46).*
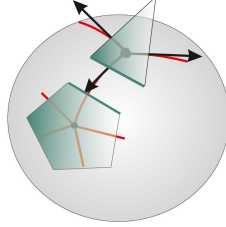
54

Figure 45: Patching.

Algorithm 30. Stressed graph to support function *Conversely, given a stressed graph (G, s), the corresponding support function is retrieved as follows.*

1. *The embedded graph G yields a reduced fan Σ. We shall construct a function h which is piecewise linear with respect to Σ.*

2. *Choose one of the 3-dimensional cones σ_1 of the fan, and put h equal zero on σ_1.*

3. *Take a cone σ_2 which shares a face F with σ_1. The face corresponds to an edge e of the graph G.*

   Define the restriction of h on the cone σ_2 as

   $$h \mid_{\sigma_2} = h \mid_{\sigma_1} + s(e)\langle v, \cdot \rangle.$$

   Here again v is the unit outer normal vector to the face $\sigma_1 \cap \sigma_2$ of the cone σ_1 (see Fig. 46), $s(e)$ is the value of the stress on the edge e.

4. *Proceed taking adjacent cones one by one, in an arbitrary order.*

The proof that the algorithms work correctly is based on two observations. First we show that correctness for convex polytopes. Indeed, in this case, the adjacent cones σ_1 and σ_2 defined above correspond to two vertices of the polytope. The vertices equal the points p_1 and p_2 respectively. The length of the connecting edge (which is the value of the stress) equals exactly $|p_1 - p_2| = \langle p_1 - p_2, v \rangle$, since the vector v is the unit parallel to the edge. Moreover, because of the choice of the direction of v, it is codirected with $p_1 - p_2$. It remains to extend the statement by linearity to virtual polytopes.

Maxwell's correspondence. We now relate the previous discussion on *support functions vs. stressed graphs* to a classical result in rigidity theory concerning *3D lifting vs. stress* introduced by J. C. Maxwell in [24].

Let G be a graph embedded in the plane $\mathbb{R}^2$ such that the edges are realized as straight-line segments. The embedding induces a tiling of the plane into
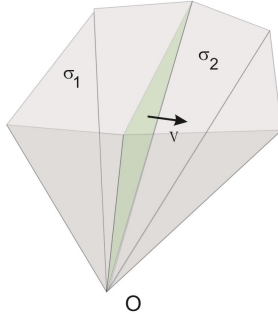
Figure 46: The normal to the common face of two adjacent cones in a fan.

regions, all but one of which are bounded. A *lifting* of an embedded graph is a continuous function $h : \mathbb{R}^2 \to \mathbb{R}$ which is piecewise linear with respect of the tiling. The graph (in other terminology, the *terrain*) of the function h is some piecewise linear surface in 3D.

Each graph has a family of *trivial liftings*, which are the (globally) linear functions. But not all have non-trivial liftings. It was James Clerk Maxwell who observed in [24] that liftability is directly related to the existence of equilibrium stress on the embedded graph. He presented a way of reconstructing a lifting from a stress and vise versa, which is referred to as *Maxwell's correspondence*. More precisely, Maxwell established a homomorphism between the linear space of liftings factorized by globally linear functions and the space of equilibrium stresses. In the above algorithms we adopt the approach used by Maxwell in proving the correspondence.

There exists yet another relationship between support functions and liftings of planar graphs. Assume we have a virtual polytope, which, as we know, comes with its support function h, also is expressed by a spherical stressed graph (G, s). We remind that the support function is linear with respect to the fan Σ associated to the polytope.

Take a plane $e \subset \mathbb{R}^3$ and intersect it with the fan. The intersection $\overline{G}$ equals the central projection of a hemispherical part of G onto the plane e. It resembles an embedded graph with the exception that (possibly) some edges go to infinity. We can extend Maxwell's lifting to this kind of objects by literally repeating the definition. Then the restriction of the support function h_K on the plane e is a lifting of $\overline{G}$.

6   Applications

In this section we demonstrate the usefulness of the theory of virtual polytope with a selection of problems and applications originating in various areas of mathematics.

6.1   A.D. Alexandrov's problem and hyperbolic virtual polytopes

We return to 3D to introduce *hyperbolic virtual polytopes* or, shortly, *hyperbolic polytopes*. This special class of virtual polytopes emerged from a number of geometry problems in the style of A. D. Alexandrov, where it has been used to provide new insights into one of his theorems concerning 3D *convex* polytopes, and to solve one of Alexandrov's long-standing conjectures.

The underlying idea for the results presented in this section is that hyperbolic polytopes, while retaining many of the properties of convex ones, lie almost at the opposite pole in terms of convexity properties. A generic virtual polytope is somewhere convex, somewhere concave, and somewhere saddle: the hyperbolic ones are totally saddle.

To make this precise, we rely on the following definition (illustrated in Fig. 47), valid in both the smooth and the piecewise linear case, for saddle surfaces.
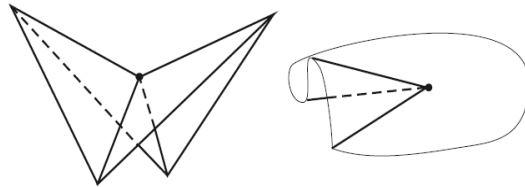
Figure 47: Saddle points on surfaces.

Definition 31. *Let F be a surface in $\mathbb{R}^3$. A point $x \in F$ is called* saddle *if no plane passing through x intersects F locally at just one point. The surface is* saddle *if all its points are saddle.*

To define hyperbolic virtual polytopes, we need the following preliminary construction. Let K be a virtual polytope in $\mathbb{R}^3$, and let h be its support function. For a vector $v \in S^2$, the equation

$$\langle x, v \rangle = 1$$

defines a plane $e(v)$. We consider the restriction of h to the plane $e(v)$ and denote by $\mathcal{F}_v$ the graph (in the sense of the "graph of a function") of this restriction. The surface $\mathcal{F}_v$ is piecewise linear. Its vertices and edges correspond to those of the fan Σ_K intersected with the open hemisphere with the pole at v.

Since convex polytopes are those virtual polytopes that have convex support function, we conclude that a virtual polytope is convex (i.e., $K \in \mathcal{P}$) if and only if the surface $\mathcal{F}_v$ is a convex surface for any v. In analogy to this property, we define:

Definition 32. *A virtual polytope K is called hyperbolic if $\mathcal{F}_v$ is a saddle surface for any $v \in S^2$.*

The theory of hyperbolic polytopes emerged originally as a tool for constructing counterexamples to the following uniqueness conjecture, proven by A.D. Alexandrov[1] in the case of analytic surfaces:

A. D. Alexandrov's conjecture: Uniqueness of smooth convex surfaces. *Let $K \subset \mathbb{R}^3$ be a smooth closed convex body, and let $R_1(x)$ and $R_2(x)$ be the principal curvature radii of its boundary ∂K at the point x. If for a constant C, at every point of ∂K, we have $R_1(x) \leq C \leq R_2(x)$, then K is a ball.*

For general smooth surfaces, the conjecture remained open for a long time, until Y. Martinez-Maure first gave a C^2 counterexample in 2001 [22]. Subsequently, G. Panina presented a series of C^∞ counterexamples and developed a systematic theory, based on hyperbolic virtual polytopes, for constructing an infinite class of such counterexamples to A. D. Alexandrov's conjecture. Details can be found in [34, 20] and further illustrations and 3D electronic models in [21].
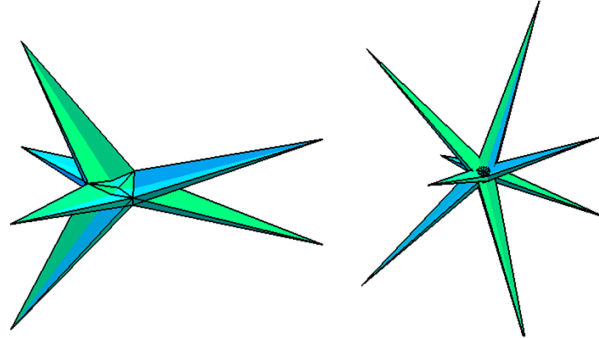

Figure 48: Two hyperbolic virtual polytopes represented by Maxwell polytopes: (left) with six *horns*, (right) with eight *horns*.

Panina's construction. To produce counter-examples to A. D. Alexandrov's conjecture, we need a simplicial hyperbolic virtual polytope with the additional property: the edges of its spherical fan are all shorter than π. Since hyperbolic

polytopes are rare phenomena among virtual polytopes, the construction of such an objects presnets the most challenging step. It can then be shown that the support function h of the constructed hyperbolic virtual polytope can be smoothened. More precisely, there exists a C^∞ smooth saddle function h' which approximates h. The smoothening technique works only for virtual polytopes with the above additional property.

We finally add to h' the support function of a large ball. Namely, let h_R be the support function of the ball of radius R. If the sum $h' + h_R$ is a convex function (for this purpose R should be sufficiently large), then $h' + h_R$ is the support function of some smooth convex body K', thus providing a counterexample to Alexandrov's conjecture.

Constructing hyperbolic polytopes. Towards this goal, we first describe a criterion for hyperbolicity of virtual polytopes.

Definition 33. *A vertex p of a spherical fan Σ is pointed, if there exists an angle larger than π incident to p. A fan is* pointed, *if all of its vertices are pointed.*

A simple sufficiency condition for a virtual polytope to be hyperbolic can now be given:

Lemma 34. *If K is a virtual polytope with a pointed spherical fan Σ_K, then it is hyperbolic.*

Example. The *hyperbolic tetrahedron* in Figure 40(b) is a hyperbolic virtual polytope. However, it cannot serve as a base for constructing counterexamples, since its fan has edges that are longer than π.

Advanced examples of hyperbolic virtual polytopes appeared in [34], and [20]. They are represented by explicitly described Maxwell polytopes with trivalent spherical fans. We have seen in Section 5 that having a trivalent spherical fan implies that the corresponding Maxwell polytope is a simplicial surface. The construction here follows the same idea of retrieving a virtual polytope via a simplicial surface: we first describe a simplicial surface (which happens to be quite complicated, with multiple self-intersections), and then retrieve its fan. Lemma 34 implies that the virtual polytope thus constructed is hyperbolic, since its fan is pointed. Figures 48 and 49 illustrate the construction.

A.D. Alexandov's uniqueness theorem for convex polytopes and its refinements. Another application of hyperbolic virtual polytopes comes from [34], and is related to the following theorem considered by A.D. Alexandrov as a discrete counterpart of the aforementioned conjecture.

Theorem 35. Uniqueness theorem for convex polytopes [1]. *Let K and M be 3-dimensional convex polytopes. If for any pair of their parallel facets,*
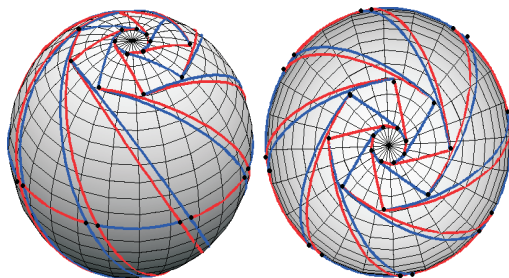
Figure 49:   Fan of the hyperbolic polytope with eight horns.

none of the facets can be placed strictly into another via a translation, then the polytopes coincide up to a translation.

Since this theorem is related to A.D. Alexandrov's conjecture, it is not surprizing that it has a natural interpretation in terms of hyperbolic polytopes. Advanced properties of hyperbolic polytopes lead to the following two refinements.

Theorem 36. *[36]. There exist two different 3-dimensional convex polytopes K and L such that for any pair of their parallel facets, there is **at most** one translation which places one of them strictly into another.*

The example is far from trivial. For its construction, we need a hyperbolic polytope with an additional property: its fan admits a regular triangulation without Steiner points (that is, without adding extra vertices).

Theorem 37. *[36] Let K, M be 3-dimensional convex polytopes satisfying the following properties, for each pair of parallel facets: (1) There exists **at most one** translation t placing the facet of K into the facet of L, and (2) There exists **no** translation t placing the facet of L into the facet of K. Then the polytopes coincide up to a translation.*

Another recent result in this direction comes from [38], and describes two convex polytopes in $\mathbb{R}^3$ such that for each pair of parallel facets, the facets are different, and there exists **exactly one** translation placing one of the facets into the other.

Hyperbolic virtual polytopes and pointed tilings.   There is a relationship between the theory of hyperbolic virtual polytopes and the theory of *pointed tilings* [42], which highlights the above constructions. Planar pointed tilings (defined below) are opposite to more traditional convex graph embeddings by being as non-convex as possible. As an analogous phenomenon, hyperbolic virtual polytopes also are as non-convex as possible. We sketch now the similarities between the two theories; further details can be found in [37].

A *pseudotriangle* is a simple polygon with exactly three angles smaller than π. All other angles are reversed. Originally, a pseudotriangle is defined to be a planar polygon, but the definition extends to spherical polygons as well. A *pseudotriangulation* is a partition of a region of the plane (or of the sphere) into pseudotriangles. A *pointed tiling* is a tiling such that each vertex has an adjacent reverse angle. Alternatively, a pointed pseudotriangulation on the plane can be defined as a finite non-crossing collection of line segments, such that at each vertex there is an adjacent reverse angle, and such that no line segments can be added between any two existing vertices while preserving this property.

Pointed pseudotriangulations on the plane were first considered by I. Streinu [45], [46] as part of her solution to the Carpenter's Ruler problem, a proof that any simple polygonal path in the plane can be straightened out by a sequence of continuous motions. A crucial property used by I. Streinu in the proof is that a pointed tiling has only the trivial stress. The pointed pseudotriangulations satisfy the conditions defining *Laman graphs*: they have exactly $2v - 3$ edges, and their k-vertex subgraphs have at most $2k-3$ edges. This follows from simple Euler counts. Laman graphs are graphs which *generically* have only the trivial stress, but may support non-trivial stress in non-generic situations. However I. Streinu showed that the pointed pseudotriangulations *never* support non-trivial stress. On the other hand, simple dimension counts show that a generically embedded graph with more than $2v - 3$ edges always has a non-trivial stress.

One critical difference between spherically embedded pointed graphs and planar pointed tilings is that on the sphere we may have *pseudo-digons*, which are spherical polygons with exactly two convex angles. Thus a pointed tiling of the sphere may contain such faces, not just pseudo-triangles. Thieir presence changes the Euler counts. As a consequence, there exist pointed graphs on the sphere which have non-zero stress. It can be shown that such a graph must have at least four pseudo-digons. This allows to construct hyperbolic virtual polytopes by just drawing on the sphere a pointed graph such that its faces are either pseudo-digons or pseudo-triangles. If the number of pseudo-digons is greater than four, the graph has a non-trivial stress, and hence (by Lemma 34) gives a hyperbolic virtual polytope.

6.2 Valuations of virtual polytopes. Volume and integer points count

In the section we discuss natural extensions of translation-invariant valuations for virtual polytopes such as volume and lattice points count.

A *valuation* is a (real-valued) function $\varphi : \mathcal{P} \to \mathbb{R}$ defined on convex polytopes which is additive: whenever K_1, K_2, and $K_1 \cup K_2$ are convex polytopes, we have $\varphi(K_1 \cup K_2) = \varphi(K_1) + \varphi(K_2) - \varphi(K_1 \cap K_2)$. A *lattice valuation* is defined only for lattice polytopes, i.e., for polytopes whose vertices lie in the standard lattice $\mathbb{Z}^n \subset \mathbb{R}^n$. In the section we consider only *translation invariant valuations*, which

coincide on the polytope and any of its translates.

A valuation φ can be uniquely extended by linearity to the elements of the algebra of polytopal functions introduced in Section 4.1, as follows. Given a polytopal function

$$f = \sum \alpha_i I_{K_i}$$

we set the valuation as:

$$\varphi(f) = \sum \alpha_i \varphi(K_i)$$

Since a virtual polytope has a representation as a polytopal function, this definition allows us to consider the *valuation φ of a virtual polytope*. We first discuss the volume, which is the most common example of a valuation.

Volume of virtual polytopes. Given a virtual polytope represented as a polytopal function f, its volume is defined to be:

$$\int_{R^n} f(x)dx$$

where integration is taken with respect to the Lebesgue measure.

The volume of a virtual polytope may be negative, as illustrated in the example from Figure 20. It also may be zero, even if the polytope is degenerated to lie in an affine subspace.

Lattice points count for virtual polytopes. Starting with Pick's classical theorem [39] (see also modern presentations in [12], [15]) till the contemporary application of calculating Kontsevich volume (see [29]), lattice points appear systematically in many mathematical and computational frameworks. Lattice points in convex polytopes provide another important example of translation invariant valuations.

The valuation can be extended to the *number of (weighted) lattice points in a virtual polytope* represented as a polytopal function f by counting the lattice points with the given weights in the definition of f:

$$Q(f) = \sum_{x \in \mathbb{Z}^n} f(x)$$

For a convex polytope K, the weights are 1 for all the points of K. For a virtual polytope, the values of the weights are the values of the polytopal function f, as in the example from Figure 50.

Valuations: general case. Keeping in mind these two motivating examples, we treat now the general case of an arbitrary valuation. Let $(\lambda)K = \{\lambda x : x \in$
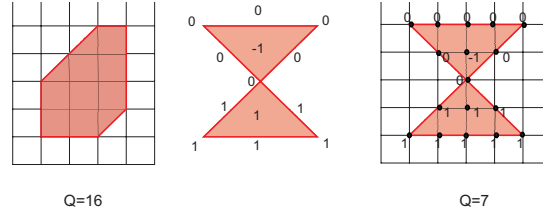
Figure 50: Integer points in a convex and in a virtual polygon.

$K\}$ be the polytope K dilated by λ. P. McMullen observed in [25] that each valuation behaves polynomially with respect to Minkowski addition:

Theorem 38. *([25]) Let $K_1, ..., K_n \subset \mathbb{R}^n$ be convex polytopes and φ be a valuation. For non-negative $\lambda_1, ..., \lambda_n$, the function*

$$P_\varphi(\lambda_1, ..., \lambda_n) = \varphi((\lambda_1)K_1 \otimes ... \otimes (\lambda_n)K_n)$$

is a polynomial in variables $\lambda_1, ..., \lambda_n$.

For lattice valuations, the statement is true for lattice polytopes.

If we apply it for the volume valuation V, we arrive at the classical notion of mixed volume:

Definition 39. *The coefficient of the polynomial P_φ at the monomial $\lambda_1 \cdot ... \cdot \lambda_n$ in Theorem 38 applied to the volume valuation $\varphi = V$ is called the* mixed volume *of the polytopes $K_1, ..., K_n$ and is denoted by $V(K_1, ..., K_n)$.*

We emphasize that Theorem 38 applies only to convex polytopes and positive dilations. It is therefore natural to ask: **What is the meaning of $P_\varphi(\lambda_1, ..., \lambda_n)$ for arbitrary (not all positive) $\lambda_1, ..., \lambda_n$?** Virtual polytope theory provides an elegant answer. The first observation in this direction is due to P. McMullen:

Theorem 40. *[25] Let φ be a translation-invariant valuation, let $K_1 = K_2 = ... = K_n = K$ be a convex polytope, and let P_φ be the polynomial from Theorem 38. Then*

$$P_\varphi(-1) = \sum_F (-1)^{dim F} \varphi(F),$$

where the sum extends over all faces of K including the polytope K.

In terms of virtual polytopes, this theorem can be reformulated as:

Theorem 41. *In the notation of Theorem 40, we have:*

$$P_\varphi(-1) = \varphi(K^{\otimes -1})$$

where $K^{\otimes -1}$ is the Minkowski inverse to the polytope K.

63

Taking for $\varphi = Q$, the weighted number of lattice points, this formula becomes:

$$P_Q(-1) = (-1)^{dim\ K} \cdot (\text{number of lattice points lying strictly inside } K)$$

which is *Ehrhart's reciprocity law*, see [11].

A. Pukhlikov and A. Khovanskii proved a more general fact which covers both McMullen's theorem and Ehrhart's reciprocity law. Namely, they proved that Theorem 38 is valid for arbitrary virtual polytopes and arbitrary real coefficients. To formulate this theorem, we first define the *Minkowski power of a virtual polytope*. Observe that for a virtual polytope K and a positive integer λ, the Minkowski power

$$K^{\otimes\lambda} = \underbrace{K \otimes \cdots \otimes K}_{\lambda}$$

equals the dilation by λ of the polytope K. This motivates the following definitions:

Definition 42. Minkowski power of a virtual polytope. *For a positive (not necessarily integer) λ and a virtual polytope K, we define the dilation of K by λ to be:*

$$K^{\otimes\lambda} = (\lambda)K$$

For a negative λ and for a virtual polytope K, we define

$$K^{\otimes\lambda} = (-\lambda)K^{\otimes-1}$$

With these concepts in place, we have:

Theorem 43. *[19] Let $K_1, ..., K_n \subset \mathbb{R}^n$ be virtual polytopes. For a valuation φ and any real $\lambda_1, ..., \lambda_n$, the function*

$$P_\varphi(\lambda_1, ..., \lambda_n) = \varphi(K_1^{\otimes\lambda_1} \otimes ... \otimes K_n^{\otimes\lambda_n})$$

is a polynomial in variables $\lambda_1, ..., \lambda_n$.

The same is true for a lattice valuation, for lattice virtual polytopes and integer $\lambda_1, ..., \lambda_n$.

This theorem allows us to define mixed volumes for virtual polytopes by literally repeating Definition 39. In the notation of Theorem 43 applied for the volume valuation V:

Definition 44. *The coefficient of the polynomial P_V at the monomial $\lambda_1 \cdot ... \cdot \lambda_n$ is called the mixed volume of the virtual polytopes $K_1, ..., K_n$ and is denoted by $V(K_1, ..., K_n)$.*

This construction emphasizes again the paradigm that *virtual polytopes retain most of the properties and structures of convex ones*, except, of course, for convexity.

Historical remarks. The special case of Theorem 38 with the volume taken as valuation was known long before P. McMullen: Minkowski used it when giving the definition of mixed volumes as the coefficients of the polynomial P_V. The latter became the central part of Brunn-Minkowski theory. Details can be found in many textbooks, such as [43]. Algorithmic aspects of efficient enumeration of lattice points in polytopes are treated in [3]. This review also explains the relationship between integer points count and Todd class of toric varieties, which is not covered in the present survey. However, we mention very briefly that the classical Euler-Maclaurin formula (which involves lattice points on a segment) extends to lattice points and convex polytopes. This was developed in [18] and further generalized in [7].

6.3   Mixed volumes of virtual polytopes

In the previous section we have seen that mixed volumes were originally defined for convex polytopes. McMullen's Theorem 43 enabled the extension of the concept to virtual polytopes. In this section we pursue the generalization even further, to the set of all polytopal functions (see [14, 31]).

Definition 45. *Let $f = \sum \alpha_i I_{K_i}$ be a fixed polytopal function. The mixed volume functional associated to f and defined for arbitrary polytopal functions as parameters is defined by:*

$$V(f, *, \cdots, *) := \sum \alpha_i V(K_i, *, *, \cdots, *)$$

The entries denoted by $*$ are arbitrary polytopal functions.

We say that two polytopal functions f and f' have *the same behavior with respect to mixed volume* if for any polytopal functions $g_1, ..., g_{n-1}$, we have

$$V(f, g_1, ..., g_{n-1}) = V(f', g_1, ..., g_{n-1}).$$

It is known that a convex polytope can be uniquely reconstructed by its behavior with respect mixed volume calculation. The same holds true for virtual polytopes:

Theorem 46. *[33] Two virtual polytopes have the same behavior with respect to mixed volume if and only if they coincide.*

In both convex and virtual settings, the proof is based on the fact that mixed volume calculation reduces to a formula for $V(f, g_1, ..., g_{n-1})$ involving support function of the (virtual) polytope f. The latter is known to determine the corresponding virtual polytope uniquely.

However, the theorem holds true just for virtual polytopes, and not for arbitrary polytopal functions. A natural question arises: **To what extent is a polytopal function defined by its behavior with respect to mixed volume?**

To answer the question, we define a map Ξ from polytopal functions to virtual polytopes by setting

$$\Xi(\sum \alpha_i I_{K_i}) = \bigotimes K_i^{\otimes \alpha_i}$$

Here $K_i^{\otimes \alpha_i}$ is the Minkowski power from Definition 42. The righthand side does not depend on a representation of f as a linear combination, hence the definition of the mapping Ξ is correct. As a simple but important corollary, we obtain:

Proposition 47. *Let K be a convex polytope and $I_K = \sum_i \alpha_i I_{K_i}$ be a decomposition of its characteristic function, where K_i are convex polytopes. Then:*

$$K = \bigotimes_i K_i^{\otimes \alpha_i}$$

With these preliminaries, we can formulate:

Proposition 48. *[33] A polytopal function f and the virtual polytope $\Xi(f)$ have the same behavior with respect to mixed volume.*

Combined with Theorem 46, this immediately gives:

Theorem 49. *[33] Two polytopal functions f and g have the same behavior with respect to mixed volume if and only if the associated virtual polytopes $\Xi(f)$ and $\Xi(g)$ coincide.*

This completes the classification of how polytopal functions behave with respect the mixed volume.

6.4   Minkowski decomposition of polytopes

We turn to an application motivated by the theory of *zonotopes*. A zonotope is a convex polytope decomposable as the Minkowski sum of line segments [44]. Zonotopes appear in surprisingly diverse areas of mathematics ranging from classical convexity to universality theorems [40], (oriented) matroids [4], and many others. Zonotopes are fully characterized: a polytope is a zonotope iff all its 2-dimensional faces are centrally symmetric. The summands of a zonotope are also easily recovered: they are the edges of the zonotope. The faces of a zonotope are themselves zonotopes in a lower dimension.

A natural question is to extend zonotopes to classes of polytopes having some but not all of their properties. One interesting such class consists in d-dimensional convex polyhedra which are Minkowski sums of their $(d-1)$ faces.

Characterize the d-dimensional convex polytope which can be represented as weighted Minkowski sums of their $(d-1)$-dimensional faces, and find such a representation, when it exists.

Virtual polytopes play a special role in characterizing this class.

Lemma 50. *A d-dimensional convex polytope can be represented as the weighted Minkowski sum of its $(d-1)$-dimensional faces if and only if it can be decomposed as a Minkowski sum of virtual polytopes.*

Let K be a convex polytope K in $\mathbb{R}^d$ represented by its characteristic function I_K. We set:

$$J_K(x) = lim_{\varepsilon \to 0} \frac{1}{V_\varepsilon} \int_{B_\varepsilon(x)} I_K(t) dt$$

where $B_\varepsilon(x)$ is the ball of radius ε centered at the point x, V_ε is its volume, and the integration is against Lebesgue measure.

The function $J_K(x)$ is a polytopal function. Indeed, it is constant on the relative interiors of the faces of K, and therefore, decomposes as a weighted sum of the characteristic functions of these faces:

$$J_K(x) = \sum_F w_F I_F(x)$$

The sum ranges over all faces, including K. It is easy to verify that $w_K = 1$ and $w_F = -1/2$ for a facet F. The other weights depend on the angle measures of the polytope K. An example is provided in Figure 51.
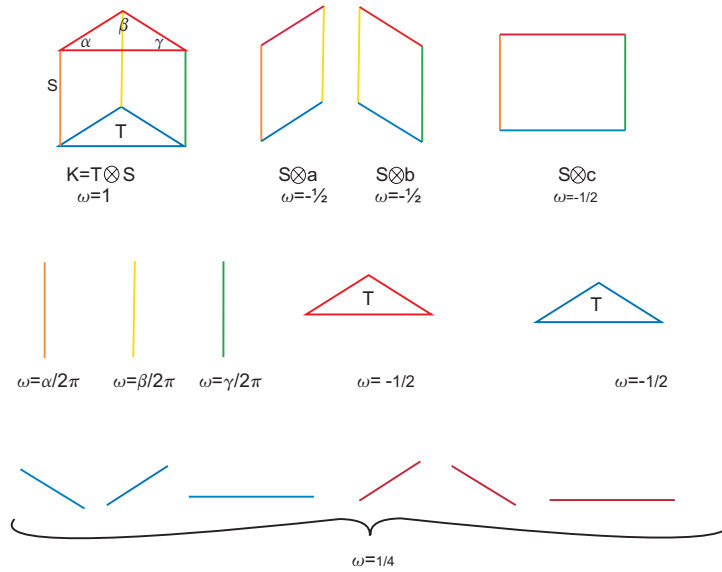

Figure 51: A prism decomposes into the sum of its faces.

Recalling that we denote by E the one-point polytope (the unit element of the group of virtual polytopes), we have:

Theorem 51. *[32] Let K be a convex d-polytope and let w_F be the weights defined as above. If the polytope K is representable as a sum of $(d-1)$-dimensional virtual polytopes, then the equality*

$$\bigotimes_F F^{\otimes w_F} = E$$

must hold, with the sum being taken over all faces, including K.

Conversely, if the above equality holds, then:

$$K = \bigotimes_F F^{\otimes -w_F}$$

Here the sum ranges over all proper faces of K (excluding K). Thus K is a Minkowski sum of virtual polytopes.

Example. A convex tetrahedron in $\mathbb{R}^3$ is not representable as a sum of 2D polytopes.

Example. We illustrate the theorem for a prism $K = T \otimes s$, which is the Minkowski sum of a triangle T and a segment s. Figure 51 lists all the faces of the prism K together with the weights. After reduction, we have

$$\bigotimes_F F^{\otimes w_F} = K \otimes s^{\otimes -1} \otimes T^{\otimes -1} = E$$

which confirms that $K = T \otimes s$.

By induction, Theorem 51 implies similar results for decomposing an d-polytope as a Minkowski sum of virtual k-polytopes for all $k < d$. This provides a complete answer to the question of Minkowski decomposability.

6.5 Projective Toric Varieties, Picard group and Riemann-Roch Theorem

We conclude our survey with a brief description of how virtual polytopes appear in the study of projective toric varieties. This was the starting point which motivated A. Khovanski and A. Pukhlikov [19] to systematically define and study them.

Projective toric varieties form an important family of algebraic varieties. The name "toric" is due to the fact that such a variety contains an algebraic torus as an open dense subset, in such a way that the action of the torus on itself extends to the entire variety. A projective toric variety is determined by the underlying fan, which is the normal fan of some lattice convex polytope. For example, the

complex projective space $\mathbb{C}P^n$ (which is a toric variety) is associated to the n-dimensional simplex.

There exists a kind of a "dictionary" which translates many algebraic geometry notions and theorems into notions and theorems from geometry of convex polytopes. These include, among others: singularities, morphisms, intersection theory, Hodge inequality and the Riemann-Roch theorem. As a consequence, general facts from algebraic geometry have implications in the theory of polytopes, and vice versa.

Virtual polytopes fit this framework nicely: the dictionary translates them as elements of the *Picard group*, which are *invertible sheaves*, whereas convex polytopes are translated as *very ample sheaves*.

Projective toric varieties. We include only a very brief overview of this topic. Detailed presentations can be found in [10], [12], and [30].

Let Σ be the outer normal fan of a convex rational polytope, i.e. a *regular rational fan* in $\mathbb{R}^n$. We denote its cones by $\sigma \in \Sigma$ and note that each cone σ induces a dual cone, denoted by $\check{\sigma}$.

A projective toric variety X_Σ is associated to Σ by the following construction:

- **Laurent polynomials.** The algebra of Laurent polynomials over $\mathbb{C}$ in n variables is:

$$\mathbb{C}[\mathbf{z}, \mathbf{z}^{-1}] = \{\sum_{\mathbf{a}} \lambda_{\mathbf{a}} \mathbf{z}^{\mathbf{a}} = \sum_{(a_1, \ldots, a_n)} \lambda_{(a_1, \ldots, a_n)} z_1^{a_1} z_2^{a_2} \ldots z_n^{a_n}\}$$

  where $\mathbf{a} = (a_1, \ldots, a_n) \in \mathbb{Z}^n$, and the coefficients $\lambda_{\mathbf{a}}$ are complex numbers.

  By definition, the support of a Laurent polynomial is:

$$supp(\sum \lambda_{\mathbf{a}} \mathbf{z}^{\mathbf{a}}) = \{\mathbf{a} : \lambda_{\mathbf{a}} \neq o\}$$

- **Defining charts.** To a cone $\sigma \in \Sigma$ we associate the algebra $R_{\check{\sigma}}$ of Laurent polynomials whose supports lie in the dual cone $\check{\sigma}$:

$$R_{\check{\sigma}} := \{f \in \mathbb{C}[z, z^{-1}] : supp(f) \subset \check{\sigma}\}.$$

- **Affine algebraic variety.** We define the affine algebraic variety $X_{\check{\sigma}}$ as the maximal spectrum of $R_{\check{\sigma}}$.

- **Gluing charts together.** The following observation allows to define gluing maps (induced by the fan) between the varieties $X_{\check{\sigma}}$. Suppose τ is a face of σ, where $\tau, \sigma \in \Sigma$. Then we have $\check{\tau} \supset \check{\sigma}$ which implies a natural inclusion map of the algebras $R_{\check{\sigma}} \to R_{\check{\tau}}$, and consequently, an inclusion

69

map of affine algebraic varieties $X_{\check{\tau}} \to X_{\check{\sigma}}$. In other words, we have an identification of $X_{\check{\tau}}$ as a subset of $X_{\check{\sigma}}$.

The collection of all $X_{\check{\sigma}}$, together with gluing mappings yields a smooth projective algebraic variety X_Σ. Because of some extra structure (it contains a dense embedded torus which acts on X_Σ), it is called a *toric variety.*

- **Structure sheaf.** The collection of algebras $\{R_{\check{\sigma}}\}$ yields a sheaf of algebras on X_Σ called the *structure sheaf* $\mathcal{O}_{X_\Sigma}$.

Picard group of X_Σ and the lattice combinatorial Picard group. The variety X_Σ comes with its *Picard group which* is the set of isomorphic classes of invertible sheaves of $\mathcal{O}_{X_\Sigma}$-modules. The group operation for invertible sheaves is the tensor product $\otimes$, the unit element in the Picard group is $\mathcal{O}_{X_\Sigma}$.

Let K be a lattice virtual polytope, i.e. a virtual polytope whose vertices lie on the standard lattice $\mathbb{Z}^n$. We assume in addition that the fan Σ_K is coarser than Σ. We represent K as an element of combinatorial Picard group, that is, as a system of translated cones $p_\sigma \otimes \check{\sigma}$, see 4.4. We define an invertible sheaf $\mathcal{F}_K$ of $\mathcal{O}_{X_\Sigma}$-modules on X_Σ by setting

$$\mathcal{F}_K(X_{\check{\sigma}}) = z^{p_\sigma} \mathcal{O}_{X_\Sigma}(X_{\check{\sigma}}).$$

Theorem 52. *[12] The map $K \to \mathcal{F}_K$ establishes an isomorphism between the lattice combinatorial Picard group $\mathcal{CP}^{\mathbb{Z}}_\Sigma$ and the Picard group of the projective toric variety X_Σ.*

Now we pass from of virtual polytopes related to one particular fan to the entire group of lattice virtual polytopes.

We have already discussed in Section 4.4 that given a fan Σ and its refinement Σ', we have natural inclusions for the groups of virtual polytopes related to the fans: $\mathcal{P}^*_\Sigma \subseteq \mathcal{P}^*_{\Sigma'}$ and $\mathcal{P}^*_{\mathbb{Z},\Sigma} \subseteq \mathcal{P}^*_{\mathbb{Z},\Sigma'}$.

Furthermore, there is a natural toric epimorphism $X_{\Sigma'} \to X_\Sigma$ which in turn induces an inclusion of the Picard groups $Pic(X_\Sigma) \subseteq Pic(X_{\Sigma'})$.

This enables us to speak of *inductive limits* of the groups $\mathcal{P}^*_\Sigma, \mathcal{P}^*_{\mathbb{Z},\Sigma}$, and $Pic(X_\Sigma)$. This means that for each of the categories we can take the union of all the groups and identify the elements via the inclusions previously described. Thus, the inductive limit in Theorem 52 yields:

Theorem 53. *The group of lattice virtual polytopes $\mathcal{P}^*_{\mathbb{Z},\Sigma}$ is isomorphic to the inductive limit of the groups $Pic(X_\Sigma)$.*

Riemann-Roch theorem and integer points enumeration. Here is one more nice observation from [17]: Theorem 38 for the valuation Q (which counts integer points) follows from the Riemann-Roch theorem for toric varieties (see [16]).

The argument proceeds by translating Theorem 38 into the language of toric varieties: a polytope K is translated as an invertible bundle, and the number of lattice points in a K is translated as the value of the Euler characteristic with coefficients in the invertible bundle corresponding to K. It remains to apply the Riemann-Roch theorem which says that the Euler characteristic behaves polynomially with respect to the tensor product.

7   Concluding remarks

The theory of virtual polytopes presented in this survey started with the very simple algebraic passage from the semigroup of convex polytopes with Minkowski addition to its associated Grothendieck group. The core of this theory lies however in the many geometric representations of virtual polytopes, together with canonical isomorphism between different representations, and in their applications.

Different problems make use of one or another of these representation, as appropriate for the particular problem. For example, the Minkowski decomposition problem presented in Section 6.4 relied on the polytopal function representation from Section 4.1. For solving the A.D. Alexandrov's problem discussed in Section 6.1, techniques on spherical stressed graphs from Section 5.1, combined with support function ideas from 5.5 were used.

An important conclusion to be extracted from this survey is that virtual polytopes posses all the properties and structures of convex polytopes except, of course, convexity. But the facial poset, mixed volumes, lattice points enumeration theory, etc. are retained by this extended class of polytopes.

Geometrically, the virtual polytopes may appear as counter-intuitive: we have seen examples of hyperbolic polytopes with everywhere saddle support function in Section 6.1, examples of a 3D virtual polytope with a not-3-connected vertex-edge graph in Example 12 and Figure 43, flexible virtual polytopes in Example 13 and Figure 44, and others.

We hope that, at the end of this survey, the reader will find, just as we did, that virtual polytopes are interesting objects to study in their own right. We anticipate that further applications will emerge in the future, some of which being of a computational nature.

References

[1] A. D. Alexandrov. On uniqueness theorems for closed surfaces (Russian). *Doklady Akad. Nauk SSSR*, 22(3):99–102, 1939.

[2] V. Alexandrov. Minkowski-type and Alexandrov-type theorems for polyhedral herissons. *Geometriae Dedicata*, 107:169–186, 2004.

[3] A. Barvinok and J. Pommersheim. An algorithmic theory of lattice points in polyhedra. In *New Perspectives in Geometric Combinatorics*, volume 38 of *MSRI Publications*. 1999.

[4] A. Björner, M. Las Vergnas, B. Sturmfels, N. White, and G. M. Ziegler. *Oriented Matroids*. Cambridge University Press, second edition, 2000.

[5] C. J. Brianchon. Théorème nouveau sur les polyèdres. *J. Ecole Polytechnique*, 15:317–319, 1837.

[6] M. Brion. The structure of the polytope algebra. *Tohoku Math. J.*, 49(1), 1997.

[7] M. Brion and M. Vergne. Lattice points in simple polytopes. *J. Amer. Math. Soc.*, 10(2):371–392, 1997.

[8] V. Buchstaber. Ring of simple polytopes and differential equations. *Proc. Steklov Inst. Math.*, 263:13–37, 2008.

[9] V. Buchstaber and N. Y. Erokhovets. Polytopes, Fibonacci numbers, Hopf algebras, and quasi-symmetric functions. *Uspekhi Mat. Nauk.*, 66:2(398):67–162, 2011.

[10] V. I. Danilov. The geometry of toric varieties. *Russian Mathematical Surveys*, 33(2):97–154, 1978.

[11] E. Erhart. *Polynomes arithmetiques et methode des polyedres en combinatoire.* Birkhauser, Basel, Stuttgart, 1977.

[12] G. Ewald. *Combinatorial convexity and algebraic geometry.* Springer Verlag, 1996.

[13] W. Fulton and B. Sturmfels. Intersection theory on toric varieties. *Topology*, 36(2):335–353, March 1997.

[14] H. Groemer. Minkowski addition and mixed volumes. *Geometriae Dedicata*, 6:141–163, 1977.

[15] B. Grünbaum. *Convex Polytopes*. John Wiley and Sons, 1967. reprinted by Springer.

[16] F. Hirzebruch. *Topological methods in algebraic geometry*. Springer-Verlag, Berlin Heidelberg New York, 1966.

[17] A. G. Khovanskii. Newton polyhedra and toroidal varieties. *Functional Analysis and Its Applications*, 11(4):289–296, 1977.

[18] A. G. Khovanskii and A. V. Pukhlikov. A Riemann-Roch theorem for integrals and sums of quasipolynomials over virtual polytopes. *Algebra and Analysis*, 4:188–216, 1992. translation in St. Petersburg Math. J., 4, 789–812, 1993.

[19] A. G. Khovanskii and A. V. Pukhlikov. Finitely additive measures of virtual polytopes. *St Petersburg Mathematical Journal*, 4(2):22 pages, 1993.

[20] M. Knyazeva and G. Panina. An illustrated theory of hyperbolic virtual polytopes. *Central European Journal of Mathematics*, 6:204–217, 2008. DOI:10.2478/s11533-008-0020-1.

[21] M. Knyazeva and G. Panina. A counterexample to A.D. Alexandrov's conjecture. EG-Models - Archive of electronic geometry models, 2010. http://www.eg-models.de/models/Surfaces/2010.02.002.

[22] Y. Martinez-Maure. Contre-example á une charactérization conjecturée de la sphére. *Comptes Rendus de l'Académie des sciences de Paris*, 332(1):41–44, 2001. Referred to in V. Alexandrov.

[23] Y. Martinez-Maure. Théorie des hérissons et polytopes. *Comptes Rendus de l'Académie des sciences de Paris*, 336:241–244, 2003.

[24] J. C. Maxwell. On reciprocal figures, frames and diagrams of forces. *Transactions of the Royal Society Edinburgh*, 26:1–40, 1870.

[25] P. McMullen. Valuations and Euler-type relations. *Proceedings of the London Mathematical Society*, s3-35(1):113–135, 1977.

[26] P. McMullen. The polytope algebra. *Advances in Mathematics*, 78(1):76–130, 1989.

[27] P. McMullen. On simple polytopes. *Invent. Math.*, 113(1):419–444, 1993.

[28] P. McMullen. Separation in the polytope algebra. *Beiträge für Algebra und Geometrie*, 34(1):15–30, 1993.

[29] P. Norbury. Counting lattice points in the moduli space of curves. arXiv:0801.4590, 2008. http://arxiv.org/abs/0801.4590.

[30] T. Oda. *Convex bodies and algebraic geometry. An introduction to the theory of toric varieties.* Ergeb. der Mathematik. Springer Verlag, 1988.

[31] G. Panina. Mixed volumes for non-convex bodies. *Journal of contemporary Mathematical Analysis*, 28(1):51–60, 1993.

[32] G. Panina. The structure of the virtual polytope group relative to cylinder subgroups. *St. Petersburg Journal of Mathematics*, 13(3):471–484, 2002. Translation, Algebra Anal. 13, No. 3, 179-197 (2002).

[33] G. Panina. Virtual polytopes and classical problems in geometry. *St. Petersburg Mathematical Journal*, 14(5):823–834, 2003. translation from Algebra Anal. 14, No. 5, 152-170,2002.

[34] G. Panina. New counter-examples to an old uniqueness hypothesis for convex bodies. *Advances in Geometry*, 5(2):301–317, 2005.

[35] G. Panina. On hyperbolic virtual polytopes and hyperbolic fans. *Central European Journal of Mathematics*, 4(2):270–293, 2006.

[36] G. Panina. A.d. alexandrov's uniqueness theorem for convex polytopes and its refinements. *Beiträge zur Algebra und Geometrie*, 49(1):59–70, 2008.

[37] G. Panina. Pointed spherical tilings and hyperbolic virtual polytopes. *Zapiski Nauchnyh seminarov POMI*, 372:157–171, 2009. http://www.mathnet.ru/links/ab80204be6fbc154881dbd8ba90bd0a2/znsl3568.pdf.

[38] G. Panina. Around A. D. Alexandrov's uniqueness theorem for convex polytopes. *Advances in Geometry*, 14(4):621–637, 2013. doi:10.1515/advgeom-2012-0006.

[39] G. A. Pick. Geometrisches zur zahlenlehre. *Sitzungsberichte des deutschen naturwissenschaftlich-medicinischen Vereines für Böhmen (Lotos) in Prag. (Neue Folge)*, 19:311–319, 1899.

[40] J. Richter-Gebert. *Realization spaces of polytopes.* Springer Verlag, 1996.

[41] L. Rodriguez and H. Rosenberg. Rigidity of certain polyhedra in R^3. *Commentarii Math Helvetici*, 75:478–503, 2000.

[42] G. Rote, F. Santos, and I. Streinu. Pseudo-triangulations: a survey. In J. E. Goodman, J. Pach, and R. Pollack, editors, *Surveys on Discrete and Computational Geometry - Twenty Years later*, volume 453 of *Contemporary Mathematics*, pages 343–410. American Mathematical Society, 2008. http://arxiv.org/abs/math/0612672.

[43] R. Schneider. *Convex Bodies: the Brunn-Minkowski Theory*, volume 44 of *Encyclopedia of Mathematics and its applications.* Cambridge University Press, Cambridge, 1993.

[44] R. Schneider and W. Weil. Zonoids and related topics. In P. M. Gruber and J. M. Wills, editors, *Convexity and Its Applications*, pages 296–317. Birkhäuser Verlag, Basel, Boston, Stuttgart, 1983.

[45] I. Streinu. A combinatorial approach to planar non-colliding robot arm motion planning. *Proc. 41st IEEE Annual Symposium on Foundations of Computer Science (FOCS)*, pages 443–453, 2000.

[46] I. Streinu. Pseudo-triangulations, rigidity and motion planning. *Discrete and Computational Geometry*, 34(4):587–635, November 2005.

[47] O. Y. Viro. Some integral calculus based on Euler characteristic. volume 1346 of *Lecture Notes in Mathematics*, pages 127–138. 1989.

[48] G. M. Ziegler. *Lectures on Polytopes.* Springer Verlag, New York, 1995.